



N série:

الجمهورية الجزائرية الديمقراطية الشعبية

République Algérienne Démocratique et Populaire

وزارة التعليم العالي والبحث العلمي

Ministère de l'Enseignement Supérieur et de la Recherche Scientifique

جامعة الشهيد حمّة لخضر الوادي

Université Echahid Hamma Lakhdar -El OUED

كلية علوم الطبيعة والحياة

Faculté des Sciences de la Nature et de la Vie

قسم البيولوجيا الخلوية والجزيئية

Département de biologie Cellulaire et Moléculaire

MEMOIRE DE FIN D'ETUDE

En vue de l'obtention du diplôme de Master Académique en Sciences

Biologiques

Spécialité : Biochimie appliquée

THEME

**In silico molecular docking evaluation of anti-covid19 activity of
potentially new ferrouquine derivatives**

Présenté Par:

ADOUANI Ali

Président : ZAIM Siham

M.A.A Université d'El Oued

Examineur : BEN ALI Abdelhai

M.C.B Université d'El Oued

Promoteur : Lanez Touhami

Professeur, Université d'El Oued

Co-Promoteur : M^{elle} ZEGHEB Nadjiba

Doctorante, Université d'El Oued

Année universitaire 2020/2021

Abstract

In this study, we aim to evaluate the activity of a new series of potentially new ferroquine derivatives towards SARS-CoV-2 using *in silico* approaches and study their effects on the main protease and the RNA polymerase of SARS-COV2. Virtual screening was performed using SwissADME and ProTox web servers. The results showed good ADMET properties for the selected compounds.

Molecular docking study showed that all compounds were active against the main protease where FQ3 and FQ 6 interacted the best with lowest binding free energy equal to -10.6 and 10.24 kcal/mol. However, only FQ16 have shown a good binding energy equal to -7.04 with RNA polymerase. The predicted IC₅₀ values were comparatively similar to the IC₅₀ of standard compounds.

Keywords: SARS-COV-2, ferroquine, main protease, RNA polymerase ADMET, Molecular docking.

Resumé

Dans cette étude, nous visons à évaluer l'activité d'une nouvelle série de dérivés de ferroquine potentiellement nouveaux contre le SARS-CoV-2 en utilisant des approches in silico et à étudier leurs effets sur la protéase et l'ARN polymérase du SARS-COV2. Le criblage virtuel a été réalisé à l'aide des serveurs web SwissADME et ProTox. Les résultats ont montré de bonnes propriétés ADMET pour les composés sélectionnés .

L'étude d'amarrage moléculaire a montré que tous les composés étaient actifs contre la protéase principale où FQ3 et FQ6 interagissaient le mieux avec une énergie libre de liaison la plus faible égale à -10,6 et 10,24 kcal/mol. Cependant, seul le FQ16 a montré une bonne énergie de liaison égale à -7,04 avec l'ARN polymérase. Les valeurs prédites de la CI50 étaient comparativement similaires à la CI50 des composés standard.

Mots clés: SARS-COV-2, ferroquine, protéase, ARN polymerase ADMET, amarrage moléculaire

المخلص:

في هذه الدراسة، نهدف إلى تقييم نشاط سلسلة جديدة من مشتقات الفيروكين الجديدة المحتملة تجاه فيروس كورونا المستجد باستخدام تقنيات *in silico* ودراسة تأثيرها على البروتياز الرئيسي وبوليميراز الحمض النووي الريبي لهذا الفيروس. تم إجراء الفحص الافتراضي باستخدام خوادم الويب SwissADME و ProTox. أظهرت النتائج خصائص ADMET جيدة للمركبات المختارة.

أظهرت دراسة الإرساء الجزيئي أن جميع المركبات كانت نشطة ضد البروتياز الرئيسي حيث تفاعل 3FQ و 6FQ بشكل أفضل مع أقل طاقة إرتباط حرة تساوي -10.6 و -10.24 كيلو كالوري / مول. ومع ذلك ، أظهر 16FQ طاقة ربط جيدة تساوي -7.04 مع بوليميريز RNA. كانت قيم 50IC المتنبأ بها متشابهة نسبياً مع 50IC للمركبات القياسية.

الكلمات الدالة: فيروس كورونا، الفيروكين، البروتياز الرئيسي، بوليميراز الحمض النووي الريبي، الارساء الجزيئي

List of Tables

Table	Legends
4.1	The Compounds of ferroquine and the Functionnel groups.
4.2	Parameters of grid
5.1	Physicochemicals Properties of compounds
5.2	Druglikness properties of compounds
5.3	Pharmacokinetiks properties of compounds
5.4	Medicinal chemistry of compounds
5.5	Toxicity prediction of compounds
5.6	Binding free energies and binding constant values obtained by molecular docking approach
5.7	Distances of formed bonds between ligands and 6LZG and 7BTF receptor's residues
5.8	Binding free energies and IC50 of standard compounds values obtained by molecular docking approach
5.9	binding free energies and IC50 of compounds values obtained by molecular docking approach.

Table of contents

ABSTRACT

LIST OF TABLES

Introduction	1
FIRST PART: Bibliographic study	2
Chapter 1: Sever Acute Respiratory syndrome coronavirus SARS-COV-2	3
1.1 SARS-COV-2 pandemic.....	4
1.2. SARS-COV-2 filiation.....	4
1.3. SARS-COV-2 syptoms.....	5
1.4. Structure and genome.....	5
1.5. The infection cycle.....	6
1.6.Spike Protein.....	7
1.7.Main protease.....	7
1.8.RNA –dependent RNA polymerase.....	8
Chapter 2:Ferrocene derivatives and ferroquine	12
2.1.Ferrocene.....	13
2.2 Ferrocene properties.....	14
2.3. Applications of ferrocene derivatives.....	14
2.4. Ferroquine.....	14
2.4.1 Structure.....	15
2.4.2 Formulation.....	15
2.4.3 Enantiomers.....	15

2.4.4 Metabolism.....	16
2.4.5 Toxicity.....	17
2.4.6 Antiviral activity.....	17
2.4.7 Mechanism of action	17
2.4.8 Cancer applications	18
Chapter 3:In silico approaches.....	19
Generality.....	20
3.1.Molecular docking.....	20
3.2. Differents types of molecular docking.....	20
3.4 Autodock molecular docking software.....	22
3.4.1 Theory of autodock.....	22
3.5.Autodock steps.....	23
3.5.1Molecular mechanics (MM).....	23
3..5.2 Quantum methods.....	24
3.5.3 Semi empirical methods.....	24
3.6. Absorption,Metabolism,Excretion,and Toxicity(ADMET).....	24
3.6.1Physicochemicals properties.....	25
3.6.2 Pharmacokinetics profile.....	27
3.6.3 Druglekiness.....	28
3.6.4 Toxicity Profile.....	29
SECOND PART: Experimental study.....	43
Chapter 4:Materials and methods.....	44
4.1 Introduction.....	45

4.2 Combinatorial Library.....	45
4.3 In silico ADMET screening.....	46
4.3.1. Screening for pharmacokinetics and druglikness.....	47
4.3.2. Screening For toxicity properties.....	47
4.4. Structural optimization.....	48
4.5. Protein selection.....	48
4.6 Molecular docking.....	49
4.7 Prediction of inhibitory concentration.....	49
References	
Chapter 5: Results and discussion.....	53
5.1. In silico ADMET screening.....	54
5.1.1 Physicochemicals properties.....	54
5.1.2 Druglikness and pharmacokinetics.....	55
5.1.3 Medicinal chemistry.....	58
5.1.4 Toxicity.....	59
5.2 Molecular docking.....	60
5.3 Prediction of inhibitory concentration.....	66
References	
Conclusion.....	70

Introduction

Throughout history, infectious diseases have caused havoc among societies. Emerging and re-emerging infectious diseases are now occurring at unprecedented speed. Over the past two decades, the emergence of coronavirus-associated diseases (SARS and MERS) inflicted global challenges to public health systems[1]. The coronavirus disease 2019 (COVID-19) pandemic, caused by the severe acute respiratory syndrome coronavirus 2 (SARS-CoV-2), poses an unprecedented global health crisis. The WHO declared COVID-19 a public health emergency of international concern on 30 January and a pandemic on 11 March 2020 this day, making it June 13, 2021, 175306598 confirmed cases and 3792777 deaths globally in the world reported to WHO[2]. It is particularly urgent to develop clinically effective therapies to contain the pandemic. The main protease (M^{pro}) and the RNA-dependent RNA polymerase (RdRP), which are responsible for the viral polyprotein proteolytic process and viral genome replication and transcription, respectively, are two attractive drug targets for SARS-CoV-2. Although its mode of action is still unknown, chloroquine has been reported to possess strong antiviral effects on the severe acute respiratory syndrome (SARS) causative agent.[82] In this context, ferroquine was evaluated for its activity against feline and human SARS coronavirus and compared to its parent drug, chloroquine. Beside its antimalarial activity, ferroquine was an effective inhibitor of SARS-CoV replication in Vero cells.

In this study, we aim to evaluate the activity of a new series of potentially new ferroquine derivatives towards SARS-CoV-2 using an *in silico* approach. It is spread over three parts, namely:

The first part is for a bibliographic study, which consists of three chapters:

- The chapter one speaks about SARS-COV-2.
- The chapter two includes a bibliographic overview of ferrocene derivatives and ferroquine.
- The chapter three exhibits the *in silico* approaches used in our study.

The second part concerns the experimental work which is divided into two chapters

- The chapter four contains the materials and methods applicable in our work.
- The chapter five shows the results and their discussion.

The work is finally completed by a conclusion deemed useful to value this work.

Part one :

The bibliographic study

Chapter 1 :

Sever Acute Respiratory Syndrom

Coronavirus 2(SARS-COV-2)

1.1 SARS-COV2 pandemic

Today, the world is taking a fresh start by leaving behind the tragedy of COVID-19 and moving forward to the era of technology and trade. When looking behind, we see that the increased urbanization, growing population and ample business and social activities between the countries and geographical areas had played a very important role in the spread of COVID-19 disease [1]. Historically, the world has successfully faced serious epidemics like Malaria, Small pox, Influenza, Cholera, Yellow fever, Leprosy, Ebola, swine flu etc. Right now, no matter the world has progressed so much but still some anomalies in human civilization exist. Like the humans have become so much sophisticated that they open themselves up to various trades, different eco systems, populations, and become more curious. As a result, they have become more vulnerable to catching strange diseases and this thing has paved the way towards the spread of most recent and life threatening COVID-19 pandemic. Fortunately ,as time is progressing, this COVID-19 pandemic has started becoming a part of the history books [2]. In the series of combat with COVID-19, a great tribute to the Public Healthcare Systems whose strategy and efforts has played a very effective role all over the world in decreasing the number of fatalities.

1.2. SARS-CoV-2 filiation

The coronavirus was first identified in the 1930s in domestic poultry. The family Coronaviridae includes four genera, alpha, beta, delta and gamma coronavirus. Before the appearance of this new coronavirus, six of them were known to cause human infections: two alphacoronaviruses (HCoV-NL63 ;HCoV-229E) and four betacoronaviruses (HCoV-OC43, HCoV-HKUI, SARS-CoV-1, And MERS-CoV)[3]. Phylogenetic analysis of coronavirus genomes revealed that SARS-CoV-2 is a new member of the beta-coronavirus genus, which also includes the coronavirus associated with severe acute respiratory syndrome (SARS-CoV-1), the Middle East Respiratory Syndrome coronavirus (MERS-CoV). The natural reservoir of SARS-CoV-2 appears to be the bat. The pangolin being its intermediate host.

To date, seven viruses of the Corona family are known to cause diseases in humans: four of them cause cold symptoms and three have recently undergone mutations that allow them to cause more serious respiratory diseases, very epidemic:

SARS-CoV (*Sever Acute Respiratory Syndrom Coronavirus*) was identified in

2002-2004, in Central Africa, as the cause of an epidemic of severe acute respiratory syndrome (SARS).

MERS-CoV (*Middle East Respiratory Syndrome*) was identified in 2012 in the

Middle East where it caused respiratory syndromes. Since then, 27 countries have reported infections with MERS-Cov.

SARS-CoV-2 is identified in late 2019 as the cause of the COVID19 disease that is believed to have started in Wuhan, China and spread throughout the world causing a pandemic that lasts to this day, making it June 13, 2021, 175306598 confirmed cases and 3792777 deaths globally in the world reported to WHO [4].

1.3. SARS-COV-2 Symptoms :

COVID-19 affects different people in different ways. Most infected people will develop mild to moderate illness and recover without hospitalization.

Most common symptoms: fever ,dry cough and tiredness.

Less common symptoms: aches ,pains ,sore throat , diarrhea , conjunctivitis , headache , loss of taste or smell , a rash on skin , or discolouration of fingers or toes.

Serious symptoms: difficulty breathing or shortness of breath , chest pain or pressure and loss of speech or movement. On average it takes 5–6 days from when someone is infected with the virus for symptoms to show, however it can take up to 14 days [5].

1.4. Structure and genome

Coronaviruses are enveloped viruses containing a single strand of unsegmented RNA, of positive polarity (which can therefore be directly translated into protein)[6]. The genome largely codes for a replicase composed of **orf1a** and **orf1b**[7] which will be translated into two polyproteins, subsequently cleaved into 16 non-structural proteins essential for viral replication.

The virus is surrounded by a lipid membrane, containing structural membrane proteins (M) and envelope (E) that interact to form the viral envelope, this layer also contains spike glycoproteins (S)[8,9], which are responsible for attachment to the host cell and membrane fusion during infection[10], the nucleic acid associated protein (RNA) forms the nucleocapsid

(N). The nucleocapsid (NC),formed by the enomic gRNA associated with the N protein[11,12],is contained in the capsid, which is itself surrounded by the envelope(Figure 1).

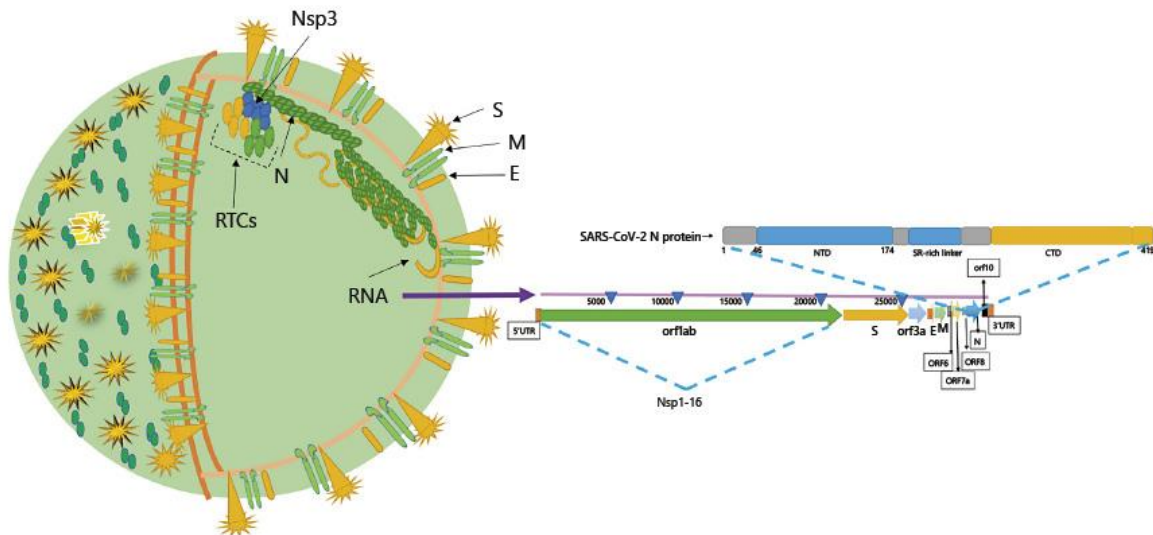


Figure 1.1:Structure of SARS-CoV-2 and its genome organization[13,14-16].

N protein is a major facilitator of viral replication within host cells, where it interacts with viral RNA during replication to form the virion after attachment to Nsp3 of the RTCs. RNA also interacts with M proteins via N. RTCs facilitate viral RNA replication. SARS-CoV-2, severe acute respiratory syndrome coronavirus-2; RTC, replication-transcription complex; Nsp, nonstructural protein; S, spike, E, envelope; M, matrix; EM, electron microscopy.

1.5.The infectious cycle

As everyone knows, knowledge is essential to understand the mode of transmission and the period of contagiousness of the virus.

The S protein of SARS-CoV-2 located on the envelope of the virus has a sufficient affinity with ACE2 (Angiotensin Converting Enzyme 2) to allow the entry of the virus into the cell [17-20]. After fusion and release of the nucleocapsid into the cytosol of the host cell. The cellular machinery translates the gene of the replicase gene into two polyproteins, which are cloned into proteins that are essential for the viral cycle, assembling into a large transcription and complex of transcription and replication. This complex will allow the production of neosynthesized viral RNA and the production of structural proteins structure of new virions. Finally the strands of RNA obtained are combined with the protein N to form the

nucleocapsid and assembly with the envelope glycoproteins allows the budding of new viral particles[21].

1.6. Spike protein

The S protein is a highly glycosylated and large type I transmembrane fusion protein that is made up of 1,160 to 1,400 amino acids, depending upon the type of virus. As compared to the M and E proteins that are primarily involved in virus assembly, the S protein plays a crucial role in penetrating host cells and initiating infection. Notably, the presence of S proteins on the coronaviruses is what gives rise to the spike-shaped protrusions found on their surface. S proteins of coronaviruses can be divided into two important functional subunits, which include the N-terminal S1 subunit, which forms the globular head of the S protein, and the C-terminal S2 region that forms the stalk of the protein and is directly embedded into the viral envelope. Upon interaction with a potential host cell, the S1 subunit will recognize and bind to receptors on the host cell, whereas the S2 subunit, which is the most conserved component of the S protein, will be responsible for fusing the envelope of the virus with the host cell membrane[22].

1.7. Main protease (M^{pro})

One of the most attractive drug targets within SARS-CoV-2 is the M^{pro} ($3CL^{pro}$) due to its vital role in processing the polyproteins translated from SARS-CoV-2 RNA. M^{pro} remains the best-characterized target protease (M^{pro} , also called $3CL^{pro}$)[23-27] along with papain-like protease(s)[28-30]. M^{pro} acts on approximately 11 cleavage locations within polyprotein 1ab. The sequence recognition at most sites consists of LQ▼(S, A, and G) (“▼” shows cleavage site). Inhibitors are likely to be nontoxic to human replication, as human proteases do not share similar cleavage specificity. The substrate-binding sites, 3C protease-like residues 10–99 and 100–182 (domains I and II) in picornavirus, are six-stranded antiparallel β -barrels that harbor the substrate between them. Residues 198–303 form domain III that consists of 5 helices that regulate the dimerization of the M^{pro} between Glu290 and Arg4 of different protomers primarily through salt bridges[31]. Amino-acids C145 and H41 form the catalytic site. The M^{pro} of SARS-CoV-2 exhibits a tight dimer that creates a contact interface between domain II and the NH₂-terminal amino acids (“N-finger”) of molecules A and B, respectively (Figure). Catalytic activity depends on the dimerization of the enzyme, as the N-finger interacts with Glu166 to facilitate the S1 pocket shape of the substrate-binding site[32].

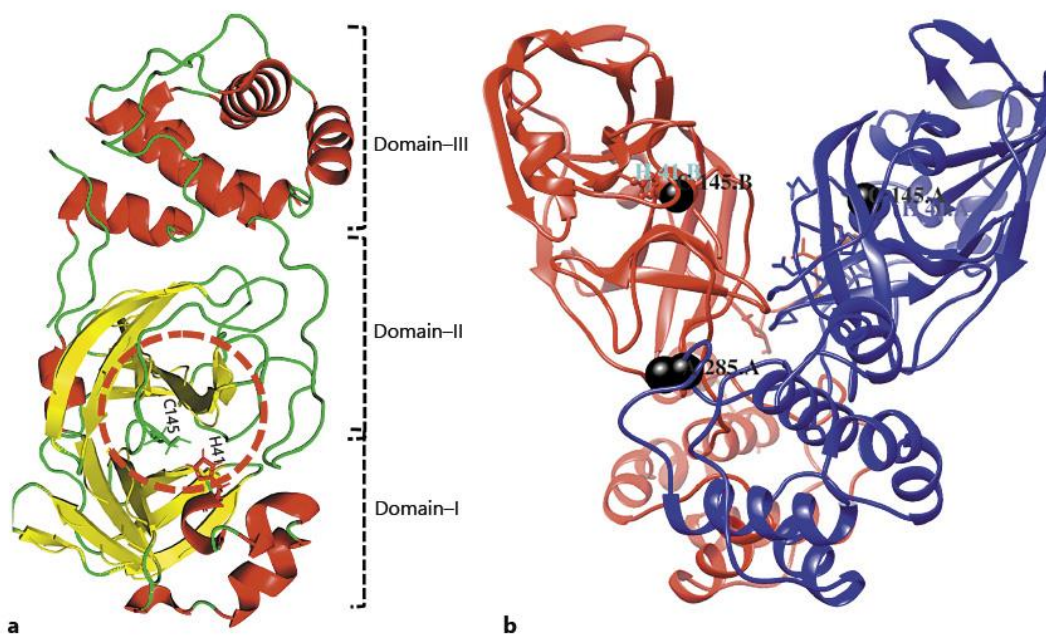


Figure 1.2: Domain organization of M^{pro} . **a** The 3 domains are shown as domain I (residues 8–101), domain II (residues 102–184), and domain III (residues 201–303). **b** Dimers. Catalytic residues (C145 and H41) are circled. In SARS-CoV-2, T285 is replaced by A285 (black balls) and Ile286 is replaced by leucine. SARS-CoV-2, severe acute respiratory syndrome coronavirus-2.

In SARS-CoV-2, residue T285 is substituted by A285, and I286 is substituted by L286 Figure1.2. Substituting S284, T285, and I286 for alanine in M^{pro} led to a threefold increase in enzymatic activity[33].

The SARS-CoVM^{pro} (T285, I286) is different from SARS-CoV-2 (A285, L286) due to the catalytic properties conferred by the residue substitutions at 285 and 286. The catalytic properties may be reduced by designing active inhibitors against these locations. Inhibitors are more likely to be toxic if they block the cleavage site (LQ▼[S, A, and G]) specific to SARS-CoV-2, as human proteases do not share a similar cleavage specificity. In a more recent study[34], two lead compounds have been synthesized (11a and 11b), targeting M^{pro} , and exhibited good activity as anti-SARS-CoV-2.

1.8.RNA-Dependent RNA polymerase

The polymerase enzymes called RNA-dependent RNA polymerase (RdRp) is playing a key role in corona viral transcription and replication assembly and thus seems as a foremost target

for antiviral drug such as remdesivir[35]. Recently, the cryo-EM structure of SARS-CoV-2 RdRp has been released in the apo form (2.8 Å resolution) and in complex (2.5 Å resolution) with a 50-base template-primer RNA and remdesivir[36]. At the central channel of the RdRp, the partial double-stranded RNA template is inserted in Figure 1.3. This insertion is basically at the first replicated base pair and terminates chain elongation, where remdesivir is covalently incorporated into the primer strand. This structure gives basic bits of knowledge into the component of viral RNA replication and a balanced format for medicate configuration to battle the viral infection.

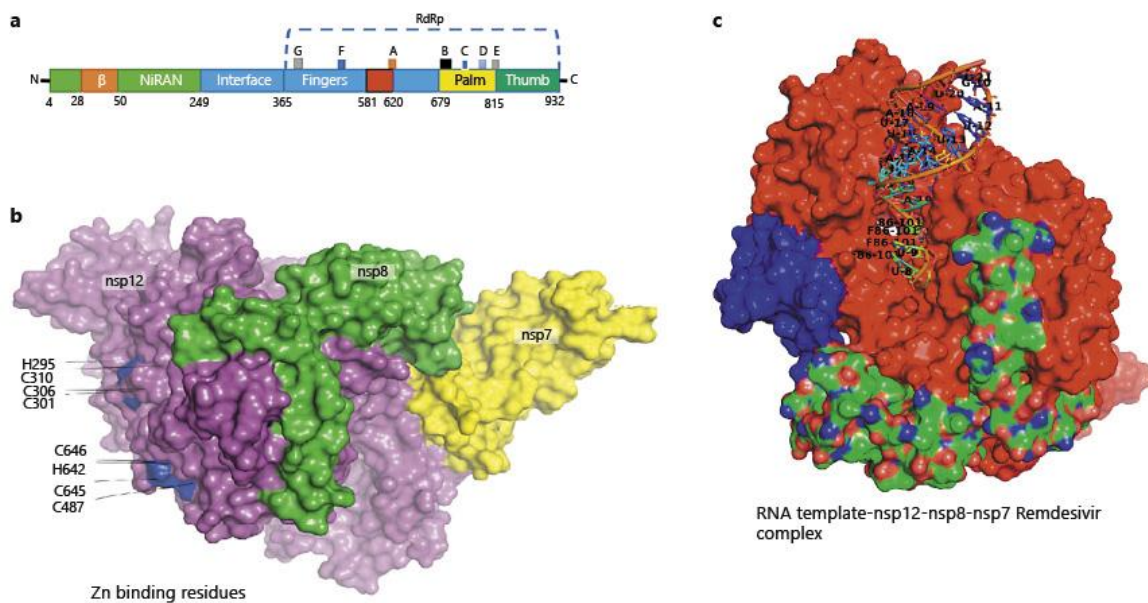


Figure 1.3 :Structure assembly of Nsp12-Nsp7-Nsp8 complex in SARS-CoV-2.

a Organization of SARS-CoV-2 domains. **b** Zn binding residues. **c** Complex structure containing active site residues for RNA template access and remdesivir (F88). SARS-CoV-2, severe acute respiratory syndrome coronavirus-2; Nsp, nonstructural protein.

The catalytic subunit (Nsp12) of an RdRp is the essential constituent of this complex. Nsp12 alone has a little action and its capacities require adornment factors including Nsp7 and Nsp8 [37], which increment RdRp template binding and processability. RdRp is likewise proposed to be the objective of a class of antiviral medications that are nucleotide analogs, including remdesivir [38]. The remdesivir is a prodrug that is converted to the active drug in the triphosphate form (RTP)[39]. The purified Nsp12 demonstrated little activity in binding to a 50-base partial double-stranded template-primer RNA[40]. The binding of Nsp12 to the template-primer RNA is dramatically expanded by the existence of Nsp7 and Nsp8.

Upon addition of adenosine triphosphate, the Nsp12-Nsp7-Nsp8 complex likewise indicated RNA polymerization activity on a poly-U template. By the addition of the active triphosphate form of remdesivir (RTP), this RNA polymerization activity was viably hindered. The apo RdRp complex is composed of unique structure that contains 1 Nsp12, 1 Nsp7, and 2 Nsp8. Unique in relation to the SARS-CoVRdRp structure, the SARS-CoV-2 RdRp structure additionally contains an N-terminal β -hairpin (residues 31–50), with 3 β -strands and 7 helices. An interface domain (residues 251–365) is subsequent the NiRAN domain and is comprised of 3 helices and 5 β -strands, which is associated with the RdRp domain (residues 366–920). The canonical cupped right-handed configuration is displayed by the Nsp12 RdRp domain, in which the finger subdomain (resides 397–581 and residues 621–679) creating a closed circle with the thumb subdomain (residues 819–920). Binding of Nsp7 and Nsp8 stabilizes the closed conformation, with 1 Nsp8 molecule sitting on the top of the finger subdomain and, furthermore, collaborating with the interface domain. The Nsp7-Nsp8 heterodimer further stabilizes the closed conformation of Nsp12, which is packed beside the thumb-finger interface. In the conserved metal-binding motifs, 2 zinc ions, which are also observed in the SARS-CoVRdRp structure have been assigned and are composed by H295, C301, C306, C310, C487, H642, C645, and C646. In keeping up the integrity of the RdRp architecture, these zinc ions likely serve as preserved structural components.

The template-RTP RdRp complex has a unique structure composed of 1 Nsp12, 1 Nsp7, and 1 Nsp8. In the final model, the second Nsp8 was not included as it was largely invisible in the EM map of the template-RTP complex. Furthermore, the template-RTP RdRp structure contains inhibitor remdesivir in its monophosphate form (RMP), and it also contains 14-base RNA in the template strand and 11-base RNA in the primer strand. At the primer strand, the inhibitor (RMP) is covalently linked, as well as 3 magnesium ions and a pyrophosphate that may attend as catalytic ions close to the active site. Although the 2 proteins (Nsp7 or Nsp8) are required for RNA binding by RdRp, surprisingly no RNA interactions are mediated by these proteins. The RMP is located at the 3' end of the primer strand, which is covalently unified into the primer strand at the +1 location. Supplementary nucleotides interrelate with residues from the back of finger subdomain at the +2 and +3 locations of the template strand. Just a single RMP is assembled into the primer strand regardless of the presence of surplus RTP in complex assembly. Accordingly, remdesivir, in the same way as other nucleotide analog prodrugs, hinders the viral RdRp activity through nonobligate RNA chain termination, a process that necessitates the transformation of the parent medication to the active

triphosphate form[41,42]. The catalytic active center is formed by the SDD sequence (residues 759–761) in motif C. At the catalytic center, both D760 and D761 are engaged in coordination of the 2 magnesium ions. The location of motifs F and G is within the finger subdomain Figure 6a and both interrelate with the template strand RNA and direct this strand into the active site. Motif F, thus, stabilizes the incoming nucleotide in the correct position for catalysis as it can interact with the primer strand RNA with the side chains of K545 and R555 contacting the +1 base. Other than remdesivir, a few nucleotide analog drugs, counting galidesivir, favipiravir, EIDD-2801, and Ribavirin, effectively hinder SARS-CoV-2 replication in cell-based measures[43,44]. These nucleotide analogs are proposed to repress the viral RdRp as remdesivir with the help of non obligate RNA chain termination, a process that necessitates the alteration of the parent compound to the triphosphate active form.

Chapter 2:

Ferrocene derivatives and
ferroquine

2.1.Ferrocene

Bis-cyclopentadienyle iron or ferrocene is an organometallic compound with the formula $(\eta^5\text{-C}_5\text{H}_5)_2\text{Fe}$, in this formula η^5 indicates that the five atoms of the C_5H_5 rings are coordinating to the iron cation, it is the prototypical metallocene, a type of organometallic chemical compounds consisting of two cyclopentadienyl rings bound on opposite sides of a central of a metal cation, such organometallic compounds are also known as ‘‘Sandwich Compound’’. The rapid growth of organometallic chemistry is often attributed to the excitement arising from the discovery of ferrocene and many other analogues.

Ferrocene was discovered by accident—thrice. The first known synthesis may have been made in the late 1940s by unknown researchers at Union Carbide, who tried to pass hot cyclopentadiene vapor through an iron pipe. The vapor reacted with the pipe wall, creating a "yellow sludge" that clogged the pipe. Years later, a sample of the sludge that had been saved was obtained and analyzed by E. Brimm, shortly after reading Kealy and Pauson's article, and was found to consist of ferrocene[45,46].

The second time was around 1950, when S. Miller, J. Tebboth, and J. Tremaine, researchers at British Oxygen, were attempting to synthesize amines from hydrocarbons and nitrogen in a modification of the Haber process. When they tried to react cyclopentadiene with nitrogen at 300 °C, at atmospheric pressure, they were disappointed to see the hydrocarbon react with some source of iron, yielding ferrocene. While they too observed its remarkable stability, they put the observation aside and did not publish it until after Pauson reported his findings[45,47,48]. In fact, Kealy and Pauson were provided with a sample by Miller et al., who confirmed that the products were the same compound[46]. In 1951, Peter L. Pauson and Thomas J. Kealy at Duquesne University attempted to prepare fulvalene ($(\text{C}_5\text{H}_4)_2$) by oxidative dimerization of cyclopentadiene (C_5H_6). To that end, they reacted the Grignard compound cyclopentadienyl magnesium bromide in diethyl ether with ferric chloride as an oxidizer. However, instead of the expected fulvalene, they obtained a light orange powder of "remarkable stability", with the formula $\text{C}_{10}\text{H}_{10}\text{Fe}$ [46,49]. Pauson and Kealy conjectured that the compound had two cyclopentadienyl groups, each with a single covalent bond from the saturated carbon atom to the iron atom[45]. However, that structure was inconsistent with then-existing bonding models and did not explain the unexpected stability of the compound, and chemists struggled to find the correct structure[48,50]. The structure was deduced and reported independently by three groups in

1952[51]. Woodward and Wilkinson deduced it by observing that ferrocene underwent reactions typical of aromatic compounds such as benzene[52]. E. Fischer deduced the structure (which he called "double cone") and also synthesized other metallocenes such as nickelocene and cobaltocene[53,54,55]. P. F. Eiland and R. Pepinsky confirmed the structure through X-ray crystallography and later by NMR[48,56-58].

When ferrocene was first discovered, its medicinal applications were not known. Ferrocene and its derivatives have found their way in medicinal chemistry. The use of ferrocene and its derivatives as bioorganometallic compounds has developed new field of research called bioorganometallic chemistry.

2.2.Ferrocene properties

It is a promising choice because it is small and can permeate cellular membranes. It is also stable in an aqueous environment which allows versatility when it comes to its derivatives. Due to Ferrocene exhibiting electrochemical behavior, it is a good candidate for drug design. Its lipophilic nature provides a favorable medium for the use of new biological applications such as anticancer and antimalarial drugs (ferrocifen, ferrocene, and ferroquine) [59].

2.3.Applications of ferrocene derivatives

Many ferrocene derivatives exhibit interesting antioxidant [60-62] cytotoxic [63-65], antitumor [66-68], antimalarial [59], antifungal [69] and DNA-cleaving activity [70]. Ferrocene derivatives are also used in regulating HIV virus which is responsible for AIDS [71].

The two most prominent derivatives which have been studied extensively for the treatment of malaria and cancer are respectively ferroquine and ferrocifen, these two potential medicaments were discovered in the 1990s. The ferrocenyl moiety in these two compounds participates in important metal-specific modes of action that contribute to the overall therapeutic efficacy of the molecules. Ferroquine is at present in phase II clinical trials and ferrocifen is in preclinical evaluation.

2.4.Ferroquine

In 1994, ferroquine [FQ, ([SSR97193](#))] was designed by Biot and co-workers at the University of Lille. Later on, it was successfully synthesized by incorporating a ferrocene unit into the

basic skeleton of cloroquine (CQ) [72]. FQ was found to be remarkably effective against CQ-resistant *P. falciparum* [73] with no observable immunotoxic effects in naive and infected young rats [74]. It acts on haematin and causes the inhibition of hemozoin formation [75]. The interesting antimalarial properties of FQ stimulated the extensive development of its analogues with the hope of increased efficacy, lower side effects and the ability to overcome resistance by malarial parasites. Presently, several classes of FQ derivatives and analogues have been prepared and tested for antimalarial properties, and interesting results have been obtained in several instances.

2.4.1. Structure

Ferroquine (FQ) is the first organometallic antimalarial drug. It contains a ferrocenyl group covalently flanked by a 4-aminoquinoline and a basic alkylamine. Ferroquine is a derivative of CQ and ferrocene[76].

2.4.2 Formulation

New drug candidates should enter the pharmaceutical development process in a crystalline state. Indeed, molecules in the amorphous state generally exhibit greater chemical instability, enhanced dissolution rates, altered mechanical properties, and greater hygroscopicity. Neutral FQ was selected for drug development, as FQ will become (di)protonated when entering the acidic environment of the stomach. Basic FQ crystallizes in the monoclinic space group $P2_1/n$ [75]. In the solid state, FQ is stabilized by a strong intramolecular hydrogen bond between the anilino nitrogen atom and the tertiary nitrogen atom of the side chain. Nevertheless, this H-bond is absent in polar solvents (such as water) or when protonated. This flip/flop H-bond may help transport of FQ through the hydrophobic membranes. Cationic FQ forms stable dimer structures not only in the solid state but also in solution[77]. This self-association process in water is singularly driven by $+\pi/+-\pi$ nonbonding interactions[77].

2.4.3 Enantiomers

FQ possesses planar chirality due to its 1,2-unsymmetrically substituted ferrocene moiety. Pure enantiomers (1'*R*)-FQ and (1'*S*)-FQ were obtained by enzymatic resolution using a biocatalyst[78]. Both optical isomers were equally active in vitro on *P. falciparum* at nanomolar concentrations. In vivo, both enantiomers were slightly less active than the racemic mixture against CQ sensitive and CQ resistant *P. vinckeivinckeii*, suggesting an

additive or a synergetic effect between both enantiomers. Moreover, (1'*R*)-FQ displayed a better curative effect than (1'*S*)-FQ suggesting different pharmacokinetic properties.

2.4.4 Metabolism

As illustrated in Figure 2.4, the metabolic pathway of FQ, based on experiments using animal and human hepatic models, has been proposed.

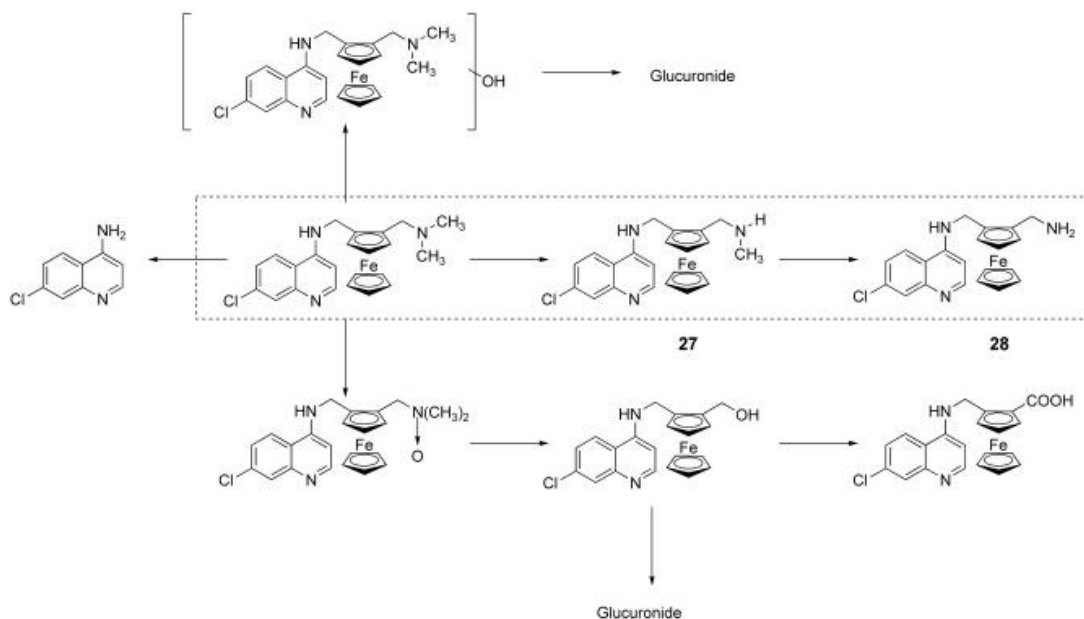


Figure 2.1: the metabolic pathway of FQ

FQ is metabolized via a major dealkylation pathway into the mono-*N*-desmethyl FQ **27** and then into di-*N,N*-desmethyl FQ **28**[79]. Other minor metabolic pathways were also identified. Cytochrome P450 isoforms 2C9, 2C19, and 3A4 and, possibly in some patients, isoform 2D6, are mainly involved in FQ oxidation.

The activity of these two main metabolites was decreased compared to that of FQ; however, the activity of the mono-*N*-desmethyl derivative **27** is significantly higher than that of CQ on both strains, and the di-*N,N*-desmethyl derivative **28** remains more active than CQ on the CQ-resistant strain[79,80].

As these two metabolites are present in significant concentrations in blood after administration of FQ, they should be involved in the global antimalarial activity of FQ.

2.4.5 Toxicity

FQ responded negatively on the Ames and FETAX (Frog Embryo Teratogenesis Assay Xenopus) tests. FQ also tested negatively in the micronucleus in vitro and in vivo assays conducted under GLP Standards. On the contrary, in the same kind of experiments, CQ was found to be weakly mutagenic and genotoxic[81].

2.4.6 Antiviral activity

Although its mode of action is still unknown, CQ has been reported to possess strong antiviral effects on the severe acute respiratory syndrome (SARS) causative agent.[82] In this context, FQ was evaluated for its activity against feline and human SARS coronavirus and compared to its parent drug, CQ. Beside its antimalarial activity, FQ was an effective inhibitor of SARS-CoV replication in Vero cells within the 1–10 μM concentration range. Nevertheless, its low selectivity index of 15 did not allow for pharmaceutical development[83].

2.4.7 Mechanism of action

The mechanism of action of FQ was studied in comparison to that of CQ. Over the years, the mechanism of CQ has been the subject of a lot of discussions and arguments. Nevertheless there is strong evidence that the action of CQ is correlated with its localization in the food vacuole of the parasite and with its association with hemozoin[84].

FQ formed a complex with hemozoin with a stoichiometry of 1 to 1[75]. The free energy of association was estimated to be -7 kcal mol^{-1} , leading to the conclusion that this non covalent interaction is weak but favorable. It was also noted that these values are similar to those previously reported for CQ. Moreover, in the presence of FQ, hemozoin is no longer converted into β -hemozoin and a dose-dependent inhibition of β -hemozoin formation was obtained. The IC_{50} of FQ was 0.8 equivalents relative to hemozoin, whereas the IC_{50} of CQ was 1.9. This clearly shows that FQ is a strong inhibitor of β -hemozoin formation, and even more potent than CQ[75].

The molecular electrostatic potential (MEP) surfaces have been computed at the DFT-B3LYP level of theory for diprotonated FQ and CQ. FQ and CQ show considerable similarity in the quinoline area. As this part of the molecule is thought to interact with hemozoin by a stacking interaction, a similar mode of interaction between these active drugs (FQ or CQ) and hemozoin was suggested[75]. At cytosolic pH, FQ was more than 100-fold more lipophilic than CQ,

whereas the difference in lipophilicity is only slight at vacuolar pH. The pK_a values of both drugs allow us to speculate that FQ accumulates at a lower concentration than CQ.

2.4.8 Cancer Applications

Cancer treatment testing was done by using cell lines that mimic the early progression of human prostate cancer were treated with FQ and induced about 60% cell death[66-68]. In vivo experiments with mice showed inhibition of tumor growth. FQ is currently undergoing clinical trials with humans and the results look promising as it is the only chloroquine derivative to have made to the second phase of development.

Chapter 3:

IN SILICO approaches

Generality

Since the early of 1980s the molecular docking[85] become the most important method used to study the interaction of a small molecule (ligand) with a macromolecule (receptor)[86] or more clearly used to predict the favorite orientation of binding between molecules[87] to have the stable complex [88] which led to predict the strength of liaisons or associations and the binding affinity between two molecules.

3.1. Molecular docking

Molecular docking is the primary method for simulation of molecular interaction. This method is able to give insights into the interaction at the atomic level, offering the opportunity to fully characterize the binding site of each molecule. Except the conformation of the complex and the orientation of the small molecule, molecular docking provides information regarding the affinity of each ligand[89]. Docking is conducted in two basic steps: first, the determination of a wide conformational area where the ligand can occupy the target with different orientations and second, the calculation of the energy associated with each conformational state[90]. Molecular docking allows to know how a ligand (small molecule) interacts with a receptor (macromolecule) and to calculate the binding energy between them. It also tells which candidate ligand will interact best with a target receptor [86,87].

The docking consists of two distinct sections. The first section consists of search algorithms, these algorithms are able to generate a large number of possible structures and to determine the binding mode. Among these algorithms: genetic algorithm, the Monte Carlo method and the second section is devoted to the function of scoring, which are mathematical methods used to estimate the interaction power and binding affinity between two molecules after have been through the docking stage. The best result for docking is the receptor-ligand adduct which have the lowest energy.

3.2. Different types of molecular docking

There are two types of molecular docking: the first type is called rigid docking which consists in obtaining the preferential conformation of a receptor-ligand system by considering each of the two molecules maintain a fixed internal geometry. In this case, the relaxation of the internal geometry of each entity, interacting in the complex, is not taken into account. However, it is quite conceivable that the receptor and ligand structures are modified during

the molecular docking process in order to optimize the interaction between the two entities, in this case, docking is called flexible docking[91].

A very large number of molecular docking software are already available. Among these, we will mention for example Autodock [92,93], MDV [111], or Hex [94] etc. They differ from each other on how to represent the molecular system and how to determine the docking score (score function). Two approaches are mainly used for modeling the receptor-ligand system. In this research project, we used the AutoDock version 4.2 software.

3.3. Theory of molecular docking

-Docking glossary

Docking: is a computational simulation of the binding of the receptor to a ligand[97].

Receptor: is the receiving molecular and it is a protein or other biopolymer [98].

Ligand: is the small molecule binds to a receptor[99]

The binding mode is the confirmation and the direction of the candidate ligand and the receptor when they joined each other [100].

The pose is the favorites (candidates) binding mod[101].

Scoring: is the calculation of the number of intramolecular interactions to delineated the correct pose [102].

Ranking: is the process of ligand classification according to its favorite of interaction with the receptor using the binding free energy[103].

-The basic theory

Two interrelated steps are employed to realize the subject of the molecular docking using computational methods[104]: the first one is a determination of binding mods by counting the number of orientations and conformations of the ligand in the active site of the receptor[105] in the second step the scoring conformation used to rank this confirmation [106]

The sampling algorithms [107] use to reproduce the binding mods and the scoring function used to classify the confirmation in increasing of the favorite interaction order[108]. Sampling algorithms : because of the enumerating conformation of ligands-receptor[109], it is so

expensive to generate computationally all the binding mods[110], this is the time to developed the samplings algorithms [111] such as Matching algorithms,LUDI, MCSS, Monte Carlo, Genetic algorithms[112], Molecular dynamics and Incremental construction for using in molecular docking software [113].

The scoring function [114] is a mathematical function used to determine the binder from inactive compounds [115] by the classification of the confirmation[116] after the calculation of binding affinity and the strong association between ligand-receptor [117] and adopting assumptions and simplifications[118].

3.4. AutoDock molecular docking software

In this software the docking is based on the trajectory simulation, is more precise:from a random initial position, outside the active site, the ligand explores the site studied by the successive repetition of movements and evaluations of the ligand-receptor interaction. The movements are performed by translation, rotation and conformational changes. The interaction energy is calculated by an energy function. The movements of the next cycle are guided by the energy variations induced by the movements of previous cycles. The algorithm stops when it finds the ideal ligand position in the receiver. These techniques take better account of the flexibility of the ligand and allow the exploration of larger regions.

3.4.1 Theory of autodock

A semiempirical free energy force field is used during the docking simulation process[95]. the force field evaluates conformation in 2 steps, the first step estimation of the intramolecular energy of transformation from the unbounded to the bounded stats of ligands receptor conformation [96], the second one is the evaluation of the intramolecular energy of combining the ligand and the receptor in the bound state[97]

$$\Delta G = \Delta G_{vdw} + \Delta G_{hbond} + \Delta G_{elec} + \Delta G_{tor} + \Delta G_{sol}$$

Where : ΔG_{vdw} is the energy of dispersion/repulsion

ΔG_{hbond} is the energy of hydrogen bonding

ΔG_{elec} is the energy of electrostatics interaction

ΔG_{tor} a term which reflects the increase in energy of the system due to the restriction of the free rotors of the ligand and the restriction of rotation and translation of the ligand during complexation at the receptor

ΔG_{solv} term related to the entropy which describes the variations of the energy of the system during the desolvation of the ligand at the time of the complexation with the receptor

3.5. Molecular modeling

In order to achieve molecular docking, the ligand structures must be optimized by molecular modeling, in what follows a theoretical insight into molecular modeling. Molecular modeling is an application of theoretical methods and computational methods to solve problems involving molecular structure and chemical reactivity. These methods can be relatively simple and usable quickly or on the contrary they can be extremely complex and require hundreds of hours of computer time, even on a super-computer. In addition, these methods often use very sophisticated in fographic means that greatly facilitate the transformation of impressive quantities of numbers into some easily interpretable graphic representations. Different approaches can be envisaged in the context of molecular modelling tools. While those of classical mechanics, which are economical in terms of computing time, make it possible to process large molecular systems, quantum methods (semi-empirical or density functional theory) are able to calculate the electronic properties of the systems. For this reason, these approaches have been used in this study.

3.5.1. Molecular mechanics (MM):

Molecular mechanics appeared in 1930 [119], but developed from 1960s, with advances in accessibility and performance of computers. It makes it possible to determine the energy of a molecule according to its atomic coordinates and to look for minima of the energy corresponding to stable conformers [120,121].

Modeling techniques based on quantum mechanics suffer from a major inconvenient: they are very expensive in terms of computation time and are therefore applicable only to molecular systems of small size. In the end, the time required to process a system by ab initio methods is approximately proportional to the fourth power of the number of electrons it contains. The use of these techniques can be problematic for the study of macromolecular objects such as an enzyme in interaction with an inhibitor or for the characterization of large-scale metallo-

organic complexes, such as those which are the subject of the invention of this research. The main idea of this method is to establish, by the choice of the energetic functions and the parameters which they contain, a mathematical model, the "field of force", which represents as well as possible the variations of the potential energy with molecular geometry. However, there is still no single model for simulating all aspects of molecular behavior, but a set of models [122].

3.5.2. Quantum methods

-The theory of the functional density (DFT):

In the formalism of the theory of the density functional the energy is expressed as a function of the electronic density. The first to express energy as a function of density was L.H. Thomas (1927), E. Fermi (1927, 1928) and P.A. Dirac (1930) on the model of non-interacting electron gas. The goal of the DFT methods is to determine functionalities that make it possible to relate electronic density to energy [123]. The DFT really started with the fundamental theorems of Hohenberg and Kohn in 1964[124], which establish a functional relation between the energy of the ground state and its electronic density. The two theorems show the existence of a density functional which makes it possible to calculate the energy of the ground state of a system.

3.5.3. Semi-empirical methods:

Semi-empirical methods are used to model large molecular systems. They are based on two approximations, the first is to consider only the valence layer (the valence electrons that intervene in the chemical bonds and thus define the properties of the system). The second cancels the multi-centre electronic repulsion integrals. Using parameters adjusted to the experimental results, they can lead sometimes to important errors in the evaluation of the total energies [125]. AutoDock based incremental docking protocol to improve docking of large ligands.

3.6. Absorption, Distribution, Metabolism, Excretion and Toxicity (ADMET) properties

Drug discovery and development is a very complex and costly attempt, which includes disease selection, target identification and validation, lead discovery and optimization, preclinical and clinical trials.

The properties of absorption, distribution, metabolism, excretion Figure 3.1, and toxicity (ADMET) are phenomena that are closely related to the fate of a chemical in the human body. Each of the properties of ADMET will reflect the outcome of a chemical compound when interacting with various organs in the body. Prediction of the ADMET properties from a compound is essential, especially for foreign chemical compounds that are consumed in the long term or large concentrations. Information about the properties of ADMET from a compound is mainly needed in the development of a new drug compound, where the information can be used to predict various pharmacokinetic phenomena of these compounds, which can then be used as necessary information in the further development of new drug compounds. Computational strategies play vital roles in early stage of drug discovery and expected to minimize the risk of toxicity. The pharmacokinetic activity and toxicity can be assessed using computational algorithms to organize, analyze, model, simulate, visualize or predict chemical toxicity. Predicted toxicity in silico is performed prior to in-vitro and in-vivo testing to minimize time and cost[126].

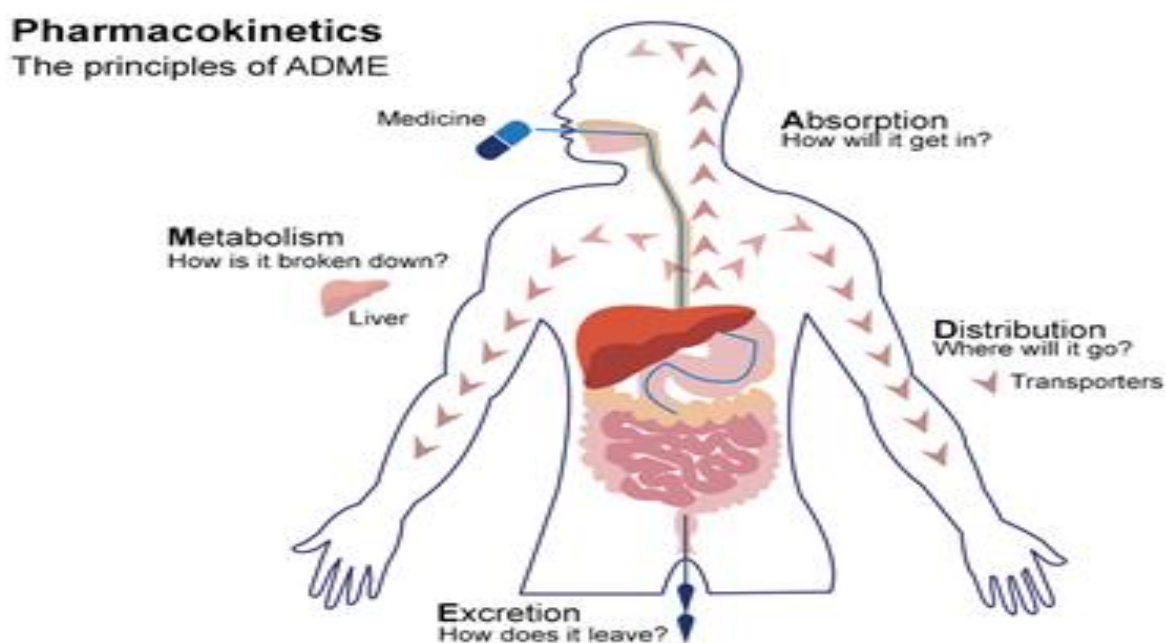


Figure 3.1: The principles of ADME.

3.6.1. Physicochemical Properties

- **Lipophilicity**

Lipophilicity, most commonly referred to as the LogP, represents the ratio at equilibrium of the concentration of a compound between two phases, an oil and a liquid phase [127].

Lipophilicity is a physicochemical parameter that has to be widely taken into account when developing new drugs since it has been reported to have a significant influence on various pharmacokinetic properties such as the absorption, distribution, permeability, as well as the routes of drugs clearance[128]. It has been increasingly demanded to develop drugs with high lipophilicity in order to fulfill the required selectivity and potency of drugs. Such demands have basically arisen as a result of the lipid nature of biological targets. On the other hand, suitable drug formulations have to reflect a good aqueous solubility as well as an acceptable degree of lipophilicity in order to assess the best oral absorption along with the required deposition and activity.

- **Hydrogen Bonding**

Hydrogen bonding is considered the driving factor that plays an obvious role in the partitioning of the biologically active compounds. Hydrogen bonding reflects the interaction between the H-bond (HB) acceptor target and the H-bond (HB) donor compound or vice versa [129].

- **Solubility**

Aqueous solubility is a fundamental property that is nearly involved in every stage of drug development due to its role in the determination of drug uptake, transfer, and elimination from the body [130]. Intrinsic solubility can be defined as the drug's thermodynamic solubility at a pH value where the drug is found to be completely in the unionized form [131]. Drugs' efficiency is primarily dependent on their aqueous solubility, therefore, drugs with poor solubility or low dissolution rates will be eliminated before entering the blood circulation and hence without giving the required pharmacological activity [130]. The solubility of chemical compounds is influenced by two important factors, namely, the lipophilicity and the tightness of the crystalline structure, and it should be noted that both parameters are related to the solubility in an inverse relationship [127]. It is also proven as a key factor in the determination of a drug's oral absorption.

- **Permeability**

Permeable drugs primarily cross biological barriers including the intestinal epithelial and the Blood Brain Barriers (BBB) by the mechanism of passive diffusion, where substances are transported by the effect of a concentration gradient. Basically, there are two types of passive

diffusion, one is the paracellular transport while the other is the transcellular transport mechanism; other drugs are being transported by either the carrier-mediated or the P-gp mediated transport [132]. Drug permeability is described by the hydrogen bonding parameter as mentioned in various studies, and the majority of results have shown that less importance is associated with hydrogen bond (HB) acceptor descriptors when predicting the permeability of the human intestinal epithelium [133].

Excretion refers to the process by which the body gets rid of the waste/toxic products. The drug excretion process can be achieved by either the kidney and/or the liver where drugs are eliminated in the form of urine or bile, respectively. The most important factor that determines the proper drug removal mechanism is the molecular weight, where substances of relatively small molecular weights are mainly removed through urine [134].

3.6.2. The pharmacokinetic profile

The pharmacokinetic profile of a drug substance is determined by various parameters including tissue distribution. The prediction of drug distribution throughout the body is basically divided into three main areas of examination, which are the BBB permeability, the volume of distribution (VD), and the plasma protein binding (PPB). All of the three areas have an observable role in the determination of drug suitable regimens, the effective plasma concentration, and the permeability across the BBB, which in turn helps in predicting CNS targets, side effects, and non-CNS therapies as well [135].

A number of aspects are being optimized during the assessment of a drug's metabolism profile at the early stages, and these aspects include the metabolic routes, stability, and interactions along with the kinetics of metabolizing enzymes as well. These aspects were shown to be essential for the selection of the suitable drug candidates during the development and discovery of pharmaceutical drugs [136]. The cytochrome P450 (CYP) is considered to be the most influential enzyme in the drug metabolism. Also essential is the knowledge about interaction of molecules with cytochromes P450 (CYP). This superfamily of isoenzymes is a key player in drug elimination through metabolic biotransformation[137]. It has been suggested that CYP and P-gp can process small molecules synergistically to improve protection of tissues and organisms[138]. One can estimate that 50 to 90% (depending on the authors) of therapeutic molecules are substrate of five major isoforms (CYP1A2, CYP2C19, CYP2C9, CYP2D6, CYP3A4) [139,140]. Inhibition of these isoenzymes is certainly one major cause of pharmacokinetics-related drug-drug interactions[141,142] leading to toxic or

other unwanted adverse effects due to the lower clearance and accumulation of the drug or its metabolites[143].

3.6.3. Drug-likeness

As defined earlier, “drug-likeness” assesses qualitatively the chance for a molecule to become an oral drug with respect to bioavailability. Bioavailability is an important property designating the quantity or fraction of the ingested dose of a chemical compound that is absorbed, and strongly influenced by the physicochemical properties of the compounds, especially by their hydrophilicity and solubility[144]. The Lipinski rule of five [145], Ghose,[146], Veber [147], Egan [148] and Muegge [149], these rules were used for drug-likeness pre-screening studies. Lipinski's Rule of Five is a rule of thumb to evaluate druglikeness, or determine if a chemical compound with a certain pharmacological or biological activity has properties that would make it a likely orally active drug in humans. The rule was formulated by Christopher A. Lipinski in 1997, based on the observation that most medication drugs are relatively small and lipophilic molecules[145]. The rule describes molecular properties important for a drug's pharmacokinetics in the human body, including their absorption, distribution, metabolism, and excretion ("ADME"). However, the rule does not predict if a compound is pharmacologically active. Lipinski's Rule of Five states that, in general, an orally active drug has:

- Not more than 5 hydrogen bond donors (OH and NH groups)
- Not more than 10 hydrogen bond acceptors (notably N and O)
- A molecular weight under 500 g/mol
- A partition coefficient $\log P$ less than 5

Note that all numbers are multiples of five, which is the origin of the rule's name.

Ghose' filter defines drug-likeness constraints as follows: calculated $\log P$ is between -0.4 and 5.6, molecular weight is between 160 and 480, molar refractivity is between 40 and 130, and the total number of atoms is between 20 and 70[146].

Veber's rule is based on the fact that majority of compounds with a good bioavailability in had less than 10 rotatable bonds (ROTB) and polar surface area less than 140 Å²[147].

The Egan rule considers good bioavailability for compounds with $0 \leq \text{TPSA} \leq 131.6 \text{ \AA}^2$ and $-1 \leq \log P \leq 5.88$ [148].

3.6.4.Toxicity Profile

In silico prediction methods that are specialized for the prediction of drugs' toxicity can be classified into methods that predict the systemic toxicity and the other methods specifically predict the toxicity for a certain organ. However, other in silico models that are concerned with predicting the carcinogenicity as well as the genotoxicity are considered to be more complicated [150].

References:

- [1] Zhu, Na, Dingyu Zhang, Wenling Wang, Xingwang Li, Bo Yang, Jingdong Song, Xiang Zhao et al. "A novel coronavirus from patients with pneumonia in China, 2019." *New England journal of medicine* (2020)..
- [2] Terada, Yutaka, Nobutaka Matsui, Keita Noguchi, Ryusei Kuwata, Hiroshi Shimoda, Takehisa Soma, Masami Mochizuki, and Ken Maeda. "Emergence of pathogenic coronaviruses in cats by homologous recombination between feline and canine coronaviruses." *PloS one* 9, no. 9 (2014): e106534.
- [4] Chiodini J. "Maps, masks and media - Traveller and practitioner resources for 2019 novel coronavirus (2019-nCoV) acute respiratory virus". *Travel medicine and infectious disease*, 33, 101574.
- [5] Khadka, Sitaram et al."Preventing COVID-19 in low- and middle-income countries." *Drugs & therapy perspectives : for rational drug selection and use*, 1-3. 13 Apr. 2020.
- [6] Batts, William N., Andrew E. Goodwin, and James R. Winton. "Genetic analysis of a novel nidovirus from fathead minnows." *Journal of general virology* 93, no. 6 (2012): 1247-1252.
- [7] Brierley, Ian, Paul Digard, and Stephen C. Inglis. "Characterization of an efficient coronavirus ribosomal frameshifting signal: requirement for an RNA pseudoknot." *Cell* 57, no. 4 (1989): 537-547.
- [8] Li, Fang. "Structure, function, and evolution of coronavirus spike proteins." *Annual review of virology* 3 (2016): 237-261.
- [9] Wrapp, Daniel, Nianshuang Wang, Kizzmekia S. Corbett, Jory A. Goldsmith, Ching-Lin Hsieh, Olubukola Abiona, Barney S. Graham, and Jason S. McLellan. "Cryo-EM structure of the 2019-nCoV spike in the prefusion conformation." *Science* 367, no. 6483 (2020): 1260-1263.
- [10] Hofmann, Heike, and Stefan Pöhlmann. "Cellular entry of the SARS coronavirus." *Trends in microbiology* 12, no. 10 (2004): 466-472.
- [11] of the International, Coronaviridae Study Group. "The species Severe acute respiratory syndrome-related coronavirus: classifying 2019-nCoV and naming it SARS-CoV-2." *Nature microbiology* 5, no. 4 (2020): 536.
- [12] Cascella, Marco, Michael Rajnik, Abdul Aleem, Scott Dulebohn, and Raffaella Di Napoli. "Features, evaluation, and treatment of coronavirus (COVID-19)." *StatPearls* (2021).

- [13] Kang, Sisi, Mei Yang, Zhongsi Hong, Liping Zhang, Zhaoxia Huang, Xiaoxue Chen, Suhua He et al. "Crystal structure of SARS-CoV-2 nucleocapsid protein RNA binding domain reveals potential unique drug targeting sites." *Acta Pharmaceutica Sinica B* 10, no. 7 (2020): 1228-1238.
- [14] Chan, Jasper Fuk-Woo, Kin-Hang Kok, Zheng Zhu, Hin Chu, Kelvin Kai-Wang To, Shuofeng Yuan, and Kwok-Yung Yuen. "Genomic characterization of the 2019 novel human-pathogenic coronavirus isolated from a patient with atypical pneumonia after visiting Wuhan." *Emerging microbes & infections* 9, no. 1 (2020): 221-236.
- [15] Tazerji, Sina Salajegheh, Phelipe Magalhães Duarte, Parastoo Rahimi, Fatemeh Shahabinejad, Santosh Dhakal, Yashpal Singh Malik, Awad A. Shehata et al. "Transmission of severe acute respiratory syndrome coronavirus 2 (SARS-CoV-2) to animals: an updated review." *Journal of translational medicine* 18, no. 1 (2020): 1-11.
- [16] Lu, Roujian, Xiang Zhao, Juan Li, Peihua Niu, Bo Yang, Honglong Wu, Wenling Wang et al. "Genomic characterisation and epidemiology of 2019 novel coronavirus: implications for virus origins and receptor binding." *The lancet* 395, no. 10224 (2020): 565-574.
- [17] Wan, Yushun, Jian Shang, Rachel Graham, Ralph S. Baric, and Fang Li. "Receptor recognition by the novel coronavirus from Wuhan: an analysis based on decade-long structural studies of SARS coronavirus." *Journal of virology* 94, no. 7 (2020): e00127-20.
- [18] Yan, Renhong, Yuanyuan Zhang, Yaning Li, Lu Xia, and Qiang Zhou. "Structure of dimeric full-length human ACE2 in complex with B0AT1." *BioRxiv* (2020).
- [19] Wang, Qihui, Yanfang Zhang, Lili Wu, Sheng Niu, Chunli Song, Zengyuan Zhang, Guangwen Lu et al. "Structural and functional basis of SARS-CoV-2 entry by using human ACE2." *Cell* 181, no. 4 (2020): 894-904.
- [20] Walls, Alexandra C., Young-Jun Park, M. Alejandra Tortorici, Abigail Wall, Andrew T. McGuire, and David Veasley. "Structure, function, and antigenicity of the SARS-CoV-2 spike glycoprotein." *Cell* 181, no. 2 (2020): 281-292..
- [21] Vennema, Harry, Gert Jan Godeke, J. W. Rossen, Wim F. Voorhout, Marian C. Horzinek, D. J. Opstelten, and P. J. Rottier. "Nucleocapsid-independent assembly of coronavirus-like particles by co-expression of viral envelope protein genes." *The EMBO journal* 15, no. 8 (1996): 2020-2028
- [22] Wang, Qihui, Gary Wong, Guangwen Lu, Jinghua Yan, and George F. Gao. "MERS-CoV spike protein: targets for vaccines and therapeutics." *Antiviral research* 133 (2016): 165-177..

- [23] Anand, Kanchan, Haitao Yang, Mark Bartlam, Zihe Rao, and Rolf Hilgenfeld. "Coronavirus main proteinase: target for antiviral drug therapy." In *Coronaviruses with special emphasis on first insights concerning SARS*, pp. 173-199. Birkhäuser Basel, 2005.
- [24] Xue, Xiaoyu, Hongwei Yu, Haitao Yang, Fei Xue, Zhixin Wu, Wei Shen, Jun Li et al. "Structures of two coronavirus main proteases: implications for substrate binding and antiviral drug design." *Journal of virology* 82, no. 5 (2008): 2515-2527.
- [25] Liang, Po-Huang. "Characterization and inhibition of SARS-coronavirus main protease." *Current topics in medicinal chemistry* 6, no. 4 (2006): 361-376.
- [26] Pillaiyar, Thanigaimalai, Manoj Manickam, Vigneshwaran Namasivayam, Yoshio Hayashi, and Sang-Hun Jung. "An overview of severe acute respiratory syndrome–coronavirus (SARS-CoV) 3CL protease inhibitors: peptidomimetics and small molecule chemotherapy." *Journal of medicinal chemistry* 59, no. 14 (2016): 6595-6628.
- [27] Gan, Yi-Ru, He Huang, Yong-Dong Huang, Chun-Ming Rao, Yang Zhao, Jin-Sheng Liu, Lei Wu, and Dong-Qing Wei. "Synthesis and activity of an octapeptide inhibitor designed for SARS coronavirus main proteinase." *Peptides* 27, no. 4 (2006): 622-625.
- [28] Báez-Santos, Yahira M., Sarah E. St John, and Andrew D. Mesecar. "The SARS-coronavirus papain-like protease: structure, function and inhibition by designed antiviral compounds." *Antiviral research* 115 (2015): 21-38..
- [29] Hilgenfeld, Rolf. "From SARS to MERS: crystallographic studies on coronaviral proteases enable antiviral drug design." *The FEBS journal* 281, no. 18 (2014): 4085-4096.
- [30] Niemeyer, Daniela, Kirstin Mösbauer, Eva M. Klein, Andrea Sieberg, Robert C. Mettelman, Anna M. Mielech, Ronald Dijkman, Susan C. Baker, Christian Drosten, and Marcel A. Müller. "The papain-like protease determines a virulence trait that varies among members of the SARS-coronavirus species." *PLoS pathogens* 14, no. 9 (2018): e1007296.
- [31] Shi, Jiahai, and Jianxing Song. "The catalysis of the SARS 3C-like protease is under extensive regulation by its extra domain." *The FEBS journal* 273, no. 5 (2006): 1035-1045.
- [32] Anand, Kanchan, Gottfried J. Palm, Jeroen R. Mesters, Stuart G. Siddell, John Ziebuhr, and Rolf Hilgenfeld. "Structure of coronavirus main proteinase reveals combination of a chymotrypsin fold with an extra α -helical domain." *The EMBO journal* 21, no. 13 (2002): 3213-3224.
- [33] Lim, Liangzhong, Jiahai Shi, Yuguang Mu, and Jianxing Song. "Dynamically-driven enhancement of the catalytic machinery of the SARS 3C-like protease by the S284-T285-I286/A mutations on the extra domain." *PloS one* 9, no. 7 (2014): e101941.

- [34] Dai, Wenhao, Bing Zhang, Xia-Ming Jiang, Haixia Su, Jian Li, Yao Zhao, Xiong Xie et al. "Structure-based design of antiviral drug candidates targeting the SARS-CoV-2 main protease." *Science* 368, no. 6497 (2020): 1331-1335..
- [35] Gao, Yan, Liming Yan, Yucen Huang, Fengjiang Liu, Yao Zhao, Lin Cao, Tao Wang et al. "Structure of the RNA-dependent RNA polymerase from COVID-19 virus." *Science* 368, no. 6492 (2020): 779-782.
- [36] Yin, Wanchao, Chunyou Mao, Xiaodong Luan, Dan-Dan Shen, Qingya Shen, Haixia Su, Xiaoxi Wang et al. "Structural basis for inhibition of the RNA-dependent RNA polymerase from SARS-CoV-2 by remdesivir." *Science* 368, no. 6498 (2020): 1499-1504.
- [37] Kirchdoerfer, Robert N., and Andrew B. Ward. "Structure of the SARS-CoV nsp12 polymerase bound to nsp7 and nsp8 co-factors." *Nature communications* 10, no. 1 (2019): 1-9.
- [38] Wang, Manli, Ruiyuan Cao, Leike Zhang, Xinglou Yang, Jia Liu, Mingyue Xu, Zhengli Shi, Zhihong Hu, Wu Zhong, and Gengfu Xiao. "Remdesivir and chloroquine effectively inhibit the recently emerged novel coronavirus (2019-nCoV) in vitro." *Cell research* 30, no. 3 (2020): 269-271.
- [39] Siegel, Dustin, Hon C. Hui, Edward Doerffler, Michael O. Clarke, Kwon Chun, Lijun Zhang, Sean Neville et al. "Discovery and synthesis of a phosphoramidate prodrug of a pyrrolo [2, 1-f][triazin-4-amino] adenine C-nucleoside (GS-5734) for the treatment of Ebola and emerging viruses." (2017): 1648-1661.
- [40] Subissi, Lorenzo, Clara C. Posthuma, Axelle Collet, Jessika C. Zevenhoven-Dobbe, Alexander E. Gorbalenya, Etienne Decroly, Eric J. Snijder, Bruno Canard, and Isabelle Imbert. "One severe acute respiratory syndrome coronavirus protein complex integrates processive RNA polymerase and exonuclease activities." *Proceedings of the National Academy of Sciences* 111, no. 37 (2014): E3900-E3909.
- [41] Tchesnokov, Egor P., Joy Y. Feng, Danielle P. Porter, and Matthias Götte. "Mechanism of inhibition of Ebola virus RNA-dependent RNA polymerase by remdesivir." *Viruses* 11, no. 4 (2019): 326.
- [42] Gordon, Calvin J., Egor P. Tchesnokov, Emma Woolner, Jason K. Perry, Joy Y. Feng, Danielle P. Porter, and Matthias Götte. "Remdesivir is a direct-acting antiviral that inhibits RNA-dependent RNA polymerase from severe acute respiratory syndrome coronavirus 2 with high potency." *Journal of Biological Chemistry* 295, no. 20 (2020): 6785-6797.
- [43] Sheahan, Timothy P., Amy C. Sims, Shuntai Zhou, Rachel L. Graham, Andrea J.

Pruijssers, Maria L. Agostini, Sarah R. Leist et al. "An orally bioavailable broad-spectrum antiviral inhibits SARS-CoV-2 in human airway epithelial cell cultures and multiple coronaviruses in mice." *Science translational medicine* 12, no. 541 (2020).

[44] Lu, Chih-Chia, Mei-Yu Chen, and Yuh-Lih Chang. "Potential therapeutic agents against COVID-19: What we know so far." *Journal of the Chinese Medical Association* (2020).

[45] Werner, Helmut. "At least 60 years of ferrocene: the discovery and rediscovery of the sandwich complexes." *Angewandte Chemie International Edition* 51, no. 25 (2012): 6052-6058.

[46] Pauson, Peter L. "Ferrocene-how it all began." *Journal of Organometallic Chemistry* 637 (2001): 3-6.

[47] Miller, Samuel A., John A. Tebboth, and John F. Tremaine. "114. Di cyclopentadienyliron." *Journal of the Chemical Society (Resumed)* (1952): 632-635

[48] Laszlo, Pierre, and Roald Hoffmann. "Ferrocene: ironclad history or Rashomon tale?." *Angewandte Chemie International Edition* 39, no. 1 (2000): 123-124.

[49] Kealy, T. J., and P. L. Pauson. "A new type of organo-iron compound." *Nature* 168, no. 4285 (1951): 1039-1040.

[50] Federman Neto, Alberto, Alessandra Caramori Pelegrino, and Vitor Andre Darin. "Ferrocene: 50 years of transition metal organometallic chemistry—from organic and inorganic to supramolecular chemistry." *ChemInform* 35, no. 43 (2004): no-no.

[51] Peterson, Kirk A., Thomas B. Adler, and Hans-Joachim Werner. "Systematically convergent basis sets for explicitly correlated wavefunctions: The atoms H, He, B–Ne, and Al–Ar." *The Journal of chemical physics* 128, no. 8 (2008): 084102.

[52] Wilkinson, Geoffrey, M. Rosenblum, M. C. Whiting, and R. B. Woodward. "The structure of iron bis-cyclopentadienyl." *Journal of the American Chemical Society* 74, no. 8 (1952): 2125-2126.

[53] Pfab, W., and E. O. Fischer. "Zur Kristallstruktur der Di-cyclopentadienyl-verbindungen des zweiwertigen Eisens, Kobalts und Nickels." *Zeitschrift für anorganische und allgemeine Chemie* 274, no. 6 (1953): 316-322.

[54] Pfab, W., and E. O. Fischer. "Zur Kristallstruktur der Di-cyclopentadienyl-verbindungen des zweiwertigen Eisens, Kobalts und Nickels." *Zeitschrift für anorganische und allgemeine Chemie* 274, no. 6 (1953): 316-322.

[55] Okuda, Jun. "Ferrocene—65 Years After." *European Journal of Inorganic Chemistry* 2017, no. 2 (2017): 217-219.

- [56] Eiland, Philip Frank, and Ray Pepinsky. "X-ray examination of iron biscyclopentadienyl." *Journal of the American Chemical Society* 74, no. 19 (1952): 4971-4971.
- [57] Dunitz, J. D., and LEa Orgel. "Bis-cyclo pentadienyl Iron: a Molecular Sandwich." *Nature* 171, no. 4342 (1953): 121-122.
- [58] Dunitz, J. D., L. E. Orgel, and Alexander Rich. "The crystal structure of ferrocene." *Acta Crystallographica* 9, no. 4 (1956): 373-375..
- [59] Biot, Christophe, Nadine François, Lucien Maciejewski, Jacques Brocard, and Daniel Poulain. "Synthesis and antifungal activity of a ferrocene–fluconazole analogue." *Bioorganic & medicinal chemistry letters* 10, no. 8 (2000): 839-841.
- [60] Lanez, Touhami, and Hadia Hemmami. "Antioxidant Activities of N-ferrocenylmethyl-2-and-3-nitroaniline and Determination of their Binding Parameters with Superoxide Anion Radicals." *Current Pharmaceutical Analysis* 13, no. 2 (2017): 110-116.
- [61] Lanez, T., and M. Henni. "Antioxidant activity and superoxide anion radical interaction with 2-(ferrocenylmethylamino) benzonitrile and 3-(ferrocenylmethylamino) benzonitrile." *Journal of the Iranian Chemical Society* 13, no. 9 (2016): 1741-1748.
- [62] Mouada, H., T. Lanez, and E. Lanez. "INVESTIGATIONS OF THE BINDING PARAMETRES OF THE INTERACTION OF N'-FERROCENYLMETHYL-N'-PHENYLACETO-AND PROPIONOHYDRAZIDE WITH DNA." *Journal of Fundamental and Applied Sciences* 11, no. 2 (2019): 875-882.
- [63] Meunier, P., I. Ouattara, B. Gautheron, J. Tirouflet, D. Camboli, and J. Besancon. "Synthèse, caractérisation et propriétés cytotoxiques des premiers 'métalloécénonucléosides'." *European journal of medicinal chemistry* 26, no. 3 (1991): 351-362.
- [64] Top, Siden, Jie Tang, Anne Vessières, Danièle Carrez, Christian Provot, and Gérard Jaouen. "Ferrocenyl hydroxytamoxifen: a prototype for a new range of oestradiol receptor site-directed cytotoxics." *Chemical Communications* 8 (1996): 955-956..
- [65]Dori Z, Gershon D, Scharf Y, Fr. Demande FR, 2,598,616 (Cl. A61K31/12), 20 Nov. 1987, US Appl. 862,804, 13 May 1986; p. 13.
- [66] Koepf-Maier P, Koepf H, Neuse EW. "Ferrocenium Salts—The First Antineoplastic Iron Compounds". *Angew. Chem, Int. Edn. Engl.* 1984, 23: 456-457.
- [67]Koepf-Maier P, Koepf H. "Metallocene complexes: Organometallic antitumoragents. *Drugs Future*". 1986, 11: 297.

- [68]Lanez T, Lanez E. "A Molecular Docking Study of N-Ferrocenylmethylnitroanilines as Potential Anticancer Drugs". *International Journal of Pharmacology, Phytochemistry and Ethnomedicine*. 2016, 2: 5-12.
- [69]Itoh T, Shirakami S, Ishida N, Yamashita Y, Yoshida T, Kim H-S, Wataya Y. "Synthesis of novel ferrocenyl sugars and their antimalarial activities". *Bioorg. Med. Chem. Lett*. 2000, 10: 1657-1659.
- [70]Baldoli C, Maiorana S, Licandro E, Zinzalla G, Perdicchia D. "Synthesis of chiralchromium tricarbonyl labeled thymine PNA monomers via the Ugi reaction". *Org.Lett*. 2002, 4: 4341-4344.
- [71]Liu W, Tang Y, Bo Sun Y, Zhu H, Dong DC. "Synthesis, characterization and bioactivity determination of ferrocenyl urea derivatives". *Appl. Organometal. Chem*. 2012, 26: 189-193.
- [72]Biot C., Glorian G., Maciejewski L.A., Brocard J.S., Domarle O., Blampain G., Millet P., Georges A.J., Abessolo H., Dive D., Lebibi J. "Synthesis and antimalarial activity in vitro and in vivo of a new ferrocene-chloroquine analogue". *J. Med. Chem*. 1997;40:3715–3718.
- [73]Biot C. "Ferroquine: a new weapon in the fight against malaria". *Curr. Med. Chem. Anti-infect. Agents*. 2004;3:135–147.
- [74]Pierrot C., Lafitte S., Dive D., Fraisse L., Brocard J., Khalife J. "Analysis of immune response patterns in naive and *Plasmodium berghei*-infected young rats following a ferroquine treatment". *Int. J. Parasitol*. 2005;35:1601–1610
- [75]Biot C., Taramelli D., Forfar-Bares I., Maciejewski L.A., Boyce M., Nowogrocki G., Brocard J.S., Basilico N., Oliaro P., Egan T.J. "Insights into the mechanism of action of ferroquine. Relationship between physicochemical properties and antiplasmodial activity". *Mol. Pharm*. 2005;2:185–193.
- [76]Biot et al. "Synthesis and Antimalarial Activity in Vitro and in Vivo of a New Ferrocene–Chloroquine Analogue " [archive] *J. Med. Chem*. 1997, 40, 3715–3718.
- [77]Buisine E., de Villiers K., Egan T. J., Biot C., *J. Am. Chem. Soc*. 2006, 128, 12122–12128.
- [78]Delhaes L., Biot C., Berry L., Delcourt P., Maciejewski L. A., Camus D., Brocard J. S., Dive D., *ChemBioChem* 2002, 3, 418–423.
- [79]Daher W., Pelinski L., Klieber S., Sadoun F., Meunier V., Bourrie M., Biot C., Guillou F., Fabre G., Brocard J., Fraisse L., Maffrand J. P., Khalife J., Dive D., *Drug Metab. Dispos*. 2006, 34, 667–682.
- [80]Biot C., Delhaes L., N'Diaye C. M., Maciejewski L. A., Camus D., Dive D., Brocard J. S., *Bioorg. Med. Chem*. 1999, 7, 2843–2847.

- [81]Chatterjee T., Mukhopadhyay A., Khan K. A., Giri A. K., *Mutagenesis* 1998, 13, 619–624
- [82]Vincent M. J., Bergeron E., Benjannet S., Erickson B. R., Rollin P. E., Ksiazek T. G., Seidah N. G., Nichol S. T., *Virology* 2005, 2: 69
- [83]Biot C., Daher W., Chavain N., Fandeur T., Khalife J., Dive D., De Clercq E., *J. Med. Chem.* 2006, 49, 2845–2849
- [84]D. J. Sullivan Jr., Gluzman I. Y., Russell D. G., Goldberg D. E., *Proc. Natl. Acad. Sci. USA* 1996, 93, 11865–11870
- [85]Kuntz ID, B. J. (1982). "A geometric approach to macromolecule-ligand interactions". *J Mol Biol.*
- [86]Leonardo G. Ferreira, R. N. (2015). "Molecular Docking and Structure-Based Drug Design Strategies. *Molecules*" .
- [87]Se´rgio Filipe Sousa, P. A. (2006). "Protein–Ligand Docking: Current Status and Future Challenges". *PROTEINS: Structure, Function, and Bioinformatics* , 15–26 .
- [88]Kitchen DB, D. H. (2004). "Docking and scoring in virtual screening for drug discovery: methods and applications". *Nat Rev Drug Discov.*
- [89]McConkey et al., 2002; Meng et al., 2011
- [90]Huang and Zou, 2010;Kapetanovic, 2008
- [91]Mulliken RS. "Molecular Compounds and their Spectra. III. The Interaction of Electron Donors and Acceptors" *J. Phys. Chem.* 1952, 56 (7) : 801-822.
- [92]Globisch C, Pajeva IK, and Wiese M. "Structure-activity relationships of a series of tariquidar analogs as multidrug resistance modulators". *Bioorganic & Medicinal Chemistry*, 2006, 14(5): 1588-1598.
- [93]Oprea TI. "Chemoinformatics in Drug Discovery". 2005: J. Wiley.
- [94]Ritchie DW, and Kemp GJ. "Protein docking using spherical polar fourier correlations. *Proteins*". 2000, 39 : 178–194.
- [95]Zhiqiang Tan, I. E. (2012). "Theory of binless multi-state free energy estimation with applications to protein-ligand binding". *The Journal of Chemical Physics* .
- [96]Joost Schymkowitz, J. B. (2005). "The FoldX web server: an online force field. *Nucleic Acids Res*"
- [97]Gregory L. Warren, C. E. (2008). "Docking Algorithms and Scoring Functions; State-of-the-Art and Current Limitations. Dans R. M. Finer-Moore, *Computational and Structural Approaches to Drug Discovery Ligand–Protein Interactions*" (pp. 137-152). uk: The Royal Society of Chemistry .

- [98]Brooijmans N, K. I. (2003). "Molecular recognition and docking algorithms". *Annu Rev Biophys Biomol Struct*.
- [99]ten Brink T, E. T. (2009). "Influence of protonation, tautomeric, and stereoisomeric states on protein-ligand docking results". *J Chem Inf Model*.
- [100]Gao, H.-W. Z.-J.-Q. (2018). "Flavonoids inhibit cell proliferation and induce apoptosis and autophagy through downregulation of PI3K γ mediated PI3K/AKT/mTOR/p70S6K/ULK signaling pathway in human breast cancer cells". *Scientific Reports* .
- [101]Aumentado-Armstrong, T. (2018). "Latent Molecular Optimization for Targeted Therapeutic Design". *arXiv* , 9-18.
- [102]Zongxi Sun, Y. W. (2018). "Effects of Panax Notoginseng Saponins on Esterases Responsible for Aspirin Hydrolysis In Vitro". *Int. J. Mol. Sci*.
- [103]da Silva Figueiredo Celestino Gomes P, D. S. (2018). "Ranking docking poses by graph matching of protein-ligand interactions: lessons learned from the D3R Grand Challenge" 2. *J Comput Aided Mol Des*.
- [104]Lengauer T, R. M. (1996). "Computational methods for biomolecular docking". *Curr Opin Struct Biol*.
- [105]Lindert, S. P. (2016). "Computational methods in drug discovery". *Beilstein J. Org. Chem* .
- [106]Ramírez, D. (2016). "Computational Methods Applied to Rational Drug Design" . the open medicinal chemistry journal , 7-20.
- [107]Yves Tille, Y. T. (2006). "Sampling Algorithms. Springer Science & Business Media".
- [108]Sheng-You Huang, a. X. (2010). "Advances and Challenges in Protein-Ligand Docking". *Int. J. Mol. Sci* , 3016-3034
- [109]Tillé, Y. (2010). "XXIII Seminario Internacional de Estadística. Algorithms of sampling with equal or unequal probabilities" (pp. 1-81). University of Neuchâtel: University of Neuchâtel.
- [110]Ullrich, Y.-M. B. (2017). "Assessment of long-range-corrected exchange-correlation kernels for solids:.PACS" .
- [111]Kathryn Dempsey, K. D. (2012). "The Development of Parallel Adaptive Sampling Algorithms for Analyzing Biological Networks". *IEEE 26th International Parallel and Distributed Processing Symposium Workshops & PhD Forum* .
- [112]Akhter, M. (2016). "Challenges in Docking": Mini Review. *JSM Chemistry* .
- [113]F.H.AllenG.M.BattleS.Robertson. (2007). "The Cambridge Crystallographic Database". Dans j. B. Triggler, *Comprehensive Medicinal Chemistry II* (pp. 389-410). Elsevier Science.

- [114]Jie Liu, a. R. (2015). "Classification of Current Scoring Functions". *J. Chem. Inf. Model.* , 475-482
- [115]Huang SY, G. S. (2010). "Scoring functions and their evaluation methods for protein-ligand docking: recent advances and future directions". *Phys Chem ChemPhys.* , 899-908.
- [116]Shamsara, J. (2014). "Evaluation of 11 Scoring Functions Performance on Matrix Metalloproteinases". *International Journal of Medicinal Chemistry* .
- [117]Böhm, H.-J. (1994). "The development of a simple empirical scoring function to estimate the binding constant for a protein-ligand complex of known three-dimensional structure". *Journal of Computer-Aided Molecular Design* , 243–256
- [118]AN., J. (2006). "Scoring functions for protein-ligand docking". *Curr Protein PeptSci.* , 20-407.
- [119]Andrews DH. The Relation Between the Raman Spectra and the Structure of Organic Molecules. *Physical Review.* 1930, 36: 544
- [120]Hetényi C, Maran U. Karelson M. "A Comprehensive Docking Study on the Selectivity of Binding of Aromatic Compounds to Proteins". *Journal of chemical information and computer sciences.* 2003, 43 (5): 1576-1583.
- [121]Keseru GM. Menyhárd DK. "Role of Proximal His93 in Nitric Oxide Binding to Metmyoglobin. Application of Continuum Solvation in Monte Carlo Protein Simulations. *Biochemistry*". 1999, 38 (20): 6614-6622.
- [122]Magali T. thèse de doctorat, Université de Montpellier I. U.F.R.DE Medecine, France 2004.
- [123]Parr RG. and Yang W. "Density Functional Theory ", Oxford University Press.1989.
- [124]Hohenberg P. and Kohn W. "Density Functional Theory (DFT)". *Phys. Rev.* 1964,136, B846.
- [125]Tsiliou S, Kefala LA, Perdih F, Turel I, Kessissoglou DP, Psomas G. "Cobalt(II) complexes with non-steroidal anti-inflammatory drug tolfenamic acid: Structure and biological evaluation". *Eur. J. Med. Chem.* 2012, 48: 132-142.
- [126]Mohammad Rizki ,Fadhil Pratama, Hadi Poerwono, Siswandonno Siswodiharjo, "ADMET properties of novel 5-O-benzoylpinostrobin derivatives". *Automatically Journal of Basic and Clinical Physiology and Pharmacology.* 2019.
- [127]Bohnert, T., Prakash, C., 2012. "ADME profiling in drug discovery and development": an overview. *Encyclopedia of Drug Metabolism and Interactions* 135.
- [128]van de Waterbeemd, H., Gifford, E., 2000. "ADMET in silico modelling: towards prediction paradise?" *Nat. Rev Drug Discov.* 2 (3), 192-204

- [129]Schwoebel, J., Ebert, R., Kühne, R., Schürmann, G., 2011. "Prediction models for the Abraham hydrogen bond donor strength: comparison of semi-empirical, ab initio, and DFT methods". *J. Phys. Org. Chem.* 24
- [130]Balakin, K., Savchuk, N., Tetko, I., 2006." In silico approaches to prediction of aqueous and DMSO solubility of drug-like compounds: trends, problems and solutions". *Curr. Med. Chem.* 13 (2), 223241
- [131]Bergström, C., Charman, W. and Porter, C. 2016. "Computational prediction of formulation strategies for beyond-rule-of-5 compounds". *Adv. Drug Deliv. Rev.* 101, 621.
- [132]Hou, T., Wang, J., Zhang, W., Wang, W., Xu, X., 2006. "Recent advances in computational prediction of drug absorption and permeability in drug discovery". *Curr. Med. Chem.* 13 (22), 26532667
- [133]Refsgaard, H., Jensen, B., Brockhoff, P., Padkjær, S., Guldbandt, M., Christensen, M., 2005. "In silico prediction of membrane permeability from calculated molecular parameters". *J. Med. Chem.* 48 (3), 805811
- [134]Lamberti, G., Cascone, S., Marra, F., Titomanlio, G., d'Amore, M., Barba, A., 2016. "Gastrointestinal behavior and ADME phenomena: II. In silico simulation". *J. Drug Deliv. Sci. Technol.* 35, 165171
- [135]Lombardo, F., Gifford, E., Shalaeva, M., 2003. "In Silico ADME prediction: data, models, facts and myths". *Mini-Rev. Med. Chem.* 3 (8), 861875
- [136]Pelkonen, O., Turpeinen, M., Uusitalo, J., Rautio, A., Raunio, H., 2005. "Prediction of drug metabolism and interactions on the basis of in vitro investigations". *Basic Clin. Pharmacol. Toxicol.* 96 (3), 167175
- [137]Testa B. & Kraemer S. D. "The Biochemistry of Drug Metabolism – An Introduction - Testa - 2007 - Chemistry & Biodiversity - Wiley Online Library". *Chem. Biodivers* (2007)
- [138] van Waterschoot RA, Schinkel , "A critical analysis of the interplay between cytochrome P450 3A and P-glycoprotein: recent insights from knockout and transgenic mice". *AHParmacol Rev.* 2011 Jun; 63(2):390-410.
- [139]Wolf C. R., Smith G. & Smith R. L. "Pharmacogenetics". *British Medical Journal* (2000)
- [140]"The role of drug metabolizing enzymes in clearance". *Di L Expert Opin Drug MetabToxicol.* 2014 Mar; 10(3):379-93.
- [141]"Characteristics and common properties of inhibitors, inducers, and activators of CYP enzymes".

- [142].Huang SM, Strong JM, Zhang L, Reynolds KS, Nallani S, Temple R, Abraham S, Habet SA, Baweja RK, Burckart GJ, Chung S, Colangelo P, Frucht D, Green MD, Hepp P, Karnaukhova E, Ko HS, Lee JI, Marroum PJ, Norden JM, Qiu W, Rahman A, Sobel S, Stifano T, Thummel K, Wei XX, Yasuda S, Zheng JH, Zhao H, Lesko LJJ Clin "New era in drug interaction evaluation: US Food and Drug Administration update on CYP enzymes, transporters, and the guidance process" Pharmacol. 2008 Jun; 48(6):662-70.
- [143] Kirchmair J, Göller AH, Lang D, Kunze J, Testa B, Wilson ID, Glen RC, Schneider G, "Predicting drug metabolism: experiment and/or computation?".Nat Rev Drug Discov. 2015 Jun; 14(6):387-404.
- [144]R. P. Heaney, J. Nutr. 131 (4Supl.), 1344S–1348S (2001)
- [145]Lipinski, C. A., Lombardo, F., Dominy, B. W. & Feeney, P. J. "Experimental and computational approaches to estimate solubility and permeability in drug discovery and development settings". Adv. Drug. Deliv. Rev. **46**, 3–26 (2001).
- [146]Ghose, A. K., Viswanadhan, V. N., &Wendoloski, J. J. (1999). "A knowledge-based approach in designing combinatorial or medicinal chemistry libraries for drug discovery. 1. A qualitative and quantitative characterization of known drug databases". Journal of CombinatorialChemistry., 1(1), 55–68.
- [147]Veber, D. F., Johnson, S. R., Cheng, H.-Y., Smith, B. R., Ward, K. W., &Kopple, K. D. (2002). "Molecular properties that influence the oral bioavailability of drug candidates". Journal of Medicinal Chemistry, 45(12),2615–2623.
- [148]Egan, W. J., Merz, K. M., & Baldwin, J. J. (2000). "Prediction of drug absorption using multivariate statistics". Journal of Medicinal Chemistry,43(21), 3867–3877.
- [149]Muegge, I., Heald, S. L., &Brittelli, D. (2001). "Simple selection criteria for drug-like chemical matter". Journal of Medicinal Chemistry., 44(12),1841–1846.
- [150]Roncaglioni, A., Toropov, A., Toropova, A., Benfenati, E., 2013. "In silico methods to predict drug toxicity". Curr.Opin. Pharmacol. 13 (5), 802806

PART 2:

Experimental study

Chapter 4:

Materials and Methods

4.1.Introduction

Drug discovery is the process through which potential new therapeutic entities are identified, using a combination of computational, experimental, translational, and clinical models [151,152] Despite advances in biotechnology and understanding of biological systems, drug discovery is still a lengthy, costly, difficult, and inefficient process with a high attrition rate of new therapeutic discovery. Drug design is the inventive process of finding new medications based on the knowledge of a biological target. In the most basic sense, drug design involves the design of molecules that are complementary in shape and charge to the molecular target with which they interact and bind. Drug design frequently but not necessarily relies on computer modeling techniques and bioinformatics approaches in the big data era.

Modern drug discovery involves the identification of screening hits, medicinal chemistry and optimization of those hits to increase the affinity, selectivity (to reduce the potential of side effects), efficacy/potency, metabolic stability (to increase the half-life), and oral bioavailability. Once a compound that fulfills all of these requirements has been identified, it will begin the process of drug development prior to clinical trials.

In this study we aim to evaluate the activity of a new series of potentially new ferroquine derivatives towards SARS-CoV-2 using in silico approach. This work was performed in laboratory of Valorisation and Technology of Sahara Resources (VTRS) at university of El-Oued using the PC windows 10 with Intel Core i3 microprocessor, 4 GB memory and 64 Bit operating system.

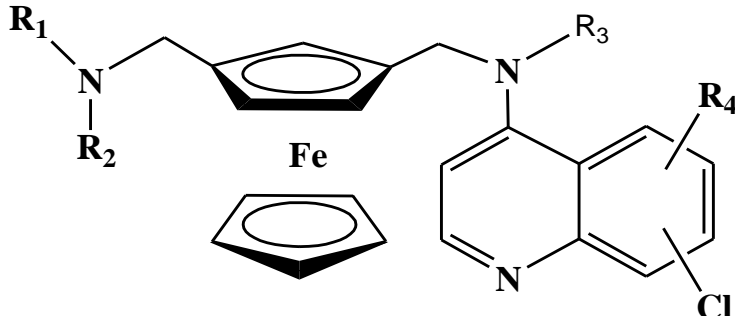
4.2.Combinatorial library

For creating combinatorial library of ferroquine,SmiLib v2.0 was used for rapid combinatorial library enumeration. SmiLib is a free, platform independent software tool for rapid combinatorial library enumeration in the flexible and portable SMILES notation. SMILES (Simplified Molecular Input Line Entry System) is a chemical notation that allows a user to represent a chemical structure in a way that can be used by the computer. SMILES is an easily learned and flexible notation.SmiLib v2.0 offers the possibility to construct very large combinatorial libraries using the flexible and portable SMILES format.The software needs three fragments,the building blocks, the scaffolds and the linkers. The ferroquine was used as scaffolds by adding the roots as shown inTable1.The functional groups

(NO₂,CN,OH,COCH₃,SCH₃) were used as building blocks, also we used an empty linker. The compounds and the functional groups were set in the SMILES format.

After the enumeration,625 compounds were created, the screening tools, SwissADME and Protox-II were used to filter the compounds depending on their ADMET properties.

Table 4.1.The Compounds of ferroquine and the Functionnel groups.



	R1	R2	R3	R4
FQ1	NO2	OH	OH	OH
FQ2	COCH3	COCH3	OH	OH
FQ3	COCH3	COCH3	OH	COCH3
FQ4	COCH3	COCH3	COCH3	COCH3
FQ5	COCH3	OH	COCH3	OH
FQ6	COCH3	OH	OH	COCH3
FQ7	COCH3	OH	OH	CN
FQ8	COCH3	OH	OH	OH
FQ9	CN	OH	OH	OH
FQ10	OH	OH	COCH3	OH
FQ11	OH	OH	OH	COCH3
FQ12	OH	OH	OH	CN
FQ13	OH	OH	OH	OH
FQ14	COCH3	OH	OH	H
FQ15	COCH3	OH	H	H
FQ16	COCH3	H	OH	CN
FQ17	H	COCH3	OH	COCH3
FQ18	COCH3	OH	COCH3	H
FQ19	COCH3	COCH3	H	OH
FQ20	OH	H	COCH3	OH

4.3.ADMET screening

The compounds were submitted to SwissADME and Protox webserver to analyze their overall drug score and toxicity risks, compared to the available drugs used[153]. The ADMET

properties including aqueous solubility, blood brain barrier (BBB), CYP binding, intestinal absorption and hepatotoxicity were evaluated for these molecules within human.

4.3.1.Screening for pharmacokinetics and drug-likeness

The website SwissADME allows to compute physicochemicals descriptors as well as to predict ADME parameters friendless of one or multiple small molecules to support drug discovery ,were performed by the online tool SwissADME [154] of Swiss Institute of Bioinformatics (<http://www.sib.swiss>) to evaluate individual ADME behaviors of those compounds [155]. 2D structural models were drawn in ChemBioDraw Ultra version 15.0 (Cambridge Software) and were then copied as SMILES to be analysed in the SwissADME webserver. The analysis task was done to check whether those compounds were inhibitor of isoforms of Cytochrome P450 (CYP) family,CYP1A2 and CYP2D6. In addition, pharmacokinetics (such as gastro intestinal absorption, P-glycoprotein and Blood brain barrier) and drug-likeness prediction Lipinski, Ghose and Veber rules and bioavailability score were evaluated [156-158]. The Lipinski, Ghose and Veber rules were applied to assess druglikeness to predict whether a compound is likely to be a bioactive according to some important parameters such as molecular weight, LogP, number of Hydrogen-bond acceptors and hydrogen-bond donnors. The SwissADME tool used vector machine algorithm (SVM) [159] with fastidiously cleaned large datasets of known inhibitors/non-inhibitors as well as substrates/non-substrates.

4.3.2 Screening For Toxicity properties :

The websever ProTox-II was used for the prediction of toxicity of chemicals, we present it that incorporates molecular similarity, pharmacophores, fragment propensities and machine-learning models for the prediction of various toxicity endpoints; such as acute toxicity, hepatotoxicity, cytotoxicity, carcinogenicity, mutagenicity, immunotoxicity, adverse outcomes pathways and toxicity targets. The predictive models are built on data from both *in vitro* assays (e.g. Tox21 assays, Ames bacterial mutation assays, hepG2 cytotoxicity assays, Immunotoxicity assays) and *in vivo* cases (e.g. carcinogenicity, hepatotoxicity).

The prediction results for the acute toxicity and toxicity targets are generated instantly. The result page will show the predicted median lethal dose (LD₅₀) in mg/kg weight, toxicity class, and prediction accuracy as well as average similarity along with three most similar toxic compounds from the dataset with the known rodent oral toxicity value. The predicted toxicity

targets information, if available will be shown with the name of the target as well as the average fit and similarity of the input compound with the pharmacophore and known ligands of the respective targets.

We choose the following very important proprieties to select the best molecules from the combinatorial library because it shows how dangerous these compounds are to the human health and their side effects:

- **Hepatotoxicity** :Drug-induced hepatotoxicity is a significant cause of acute liver failure and one of the major reasons for the withdrawal of drugs from the market[160]. Drug-induced liver injury (DILI) is either a chronic process or a rare event. However, prediction of DILI is important and one of the safety concerns for the drug developers, regulators and clinicians[161].
- **Carcinogenicity**: Chemicals that can induce tumors or increase the incidence of tumours are referred as carcinogens[162].
- **Mutagenicity**: Chemicals that cause abnormal genetic mutations such as changes in the DNA of a cell are referred as mutagens[163].Such changes can cause harm to the cells and result in certain disease, e.g. cancer.
- **Cytotoxicity** : Prediction of cytotoxicity is important to screen compounds that can cause undesired and desired cell damage, the latter as in the case of the tumour cells[164].
- **Immunotoxicity**: The adverse effect of xenobiotics on the immune system is called immunotoxicity[165].

4.4.Structural Optimization

The geometries of the studied ligands ferroquines were first optimized by molecular mechanics (MM), then they were fully re-optimized by the DFT/ B3LYP method with the 6-311G++ (d,p) basis set using Gaussian 09Wprogram package[166] using the PC windows 10 with Intel Core i7 microprocessor, 8 GB memory and 64 Bit operating system.

4.5.Protein selection

The downloading of two protein (PDB:6LU7) [167]and (PDB ID:7BTF) [168]was made from the data base Brookhaven Protein Data Bank (www.rcsb.org/pdb). The crystal structure of COVID-19 main protease (PDB:6LU7) in complex with an inhibitor N3 is obtained by X-

RAY diffraction method, and SARS-CoV-2 RNA-dependent RNA (PDB:7BTF) polymerase in complex with cofactors in reduced condition is obtained by electron microscopy method.

4.6.Molecular docking

The crystal three dimensional structures of the two proteins (PDB ID: 6LU7) and (PDB ID: 7BTF) were selected from protein data bank[169]. the targets receptors were first prepared, all water molecules, ligands and cofactors were deleted and the active site was defined using discovery studio visualize[170]. The PDB file of 6LU7 contains 2 chains for protease, so one chain C were deleted and only chain A was kept to speed up and simplify calculations. Moreover, the PDB files of 7BTF contains 4 chains (A,B,C,D) For RNA polymerase; were three chains B,C and D eliminated, so one chain A was kept to speed up and delete from it two molecules of Zinc. The PDB files of ligands were saved as PDBQT files after adding the polar hydrogen atoms. Grid boxes were generated using the AutoGrid tool, the grid parameters summarized in Table 2. For docking calculations, Lamarckian genetic algorithms were used. All docking experiments consisted of 15 docking runs with 150 individuals and 2,500,000 energy evaluations. The other parameters were left to their default values. The best conformation was selected with the lower docking energy [171,172] and was used in the docking analysis using Protein-Ligand Interaction Profiler (PLIP).

Table 4.2.Parameters of grid.

Parameter	6LU7	7BTF
Center x	-12.415	125.974
Center y	12.303	133.411
Center z	69.983	139.686
Spacing (Å)	0.375	0.4
Size (Å)	50.50.50	60.60.60

4.7. Prediction of inhibitory concentration.

To predict the IC₅₀ concentration of lead compounds, the standard inhibitors of SARS-COV (ferroquine derivatives) were docked into the same targets (SARS-CoV-2 RNA-dependent RNA and COVID-19 main protease), the binding affinity vary from -4.86 to -9.47. In 2006, a study performed by Christophe Biot et al. [175], standard inhibitors IC₅₀ including four derivatives of ferroquines F1 (1.4 mM), F2 (4.9 mM), F3 (1.9 mM) and F4 (3.6 mM). Linear regression analysis was performed through Microsoft office Excel software to generate the pIC₅₀.

References:

- [151] Zhong, Wei-Zhu, and Shu-Feng Zhou. "Molecular science for drug development and biomedicine." (2014): 20072-20078..
- [152] Xiao, Xuan, Jian-Liang Min, Wei-Zhong Lin, Zi Liu, Xiang Cheng, and Kuo-Chen Chou. "iDrug-Target: predicting the interactions between drug compounds and target proteins in cellular networking via benchmark dataset optimization approach." *Journal of Biomolecular Structure and Dynamics* 33, no. 10 (2015): 2221-2233..
- [154] Studio, Discovery. "2.1 is a product of Accelrys Inc." *San Diego, CA, USA* (2008).
- [155] Zoete, Vincent, Antoine Daina, Christophe Bovigny, and Olivier Michielin. "SwissSimilarity: a web tool for low to ultra high throughput ligand-based virtual screening." (2016): 1399-1404.
- [156] Daina, Antoine, Olivier Michielin, and Vincent Zoete. "SwissADME: a free web tool to evaluate pharmacokinetics, drug-likeness and medicinal chemistry friendliness of small molecules." *Scientific reports* 7, no. 1 (2017): 1-13.
- [157] Lipinski, Christopher A., Franco Lombardo, Beryl W. Dominy, and Paul J. Feeney. "Experimental and computational approaches to estimate solubility and permeability in drug discovery and development settings." *Advanced drug delivery reviews* 23, no. 1-3 (1997): 3-25.
- [158] Ghose, Arup K., Vellarkad N. Viswanadhan, and John J. Wendoloski. "A knowledge-based approach in designing combinatorial or medicinal chemistry libraries for drug discovery. 1. A qualitative and quantitative characterization of known drug databases." *Journal of combinatorial chemistry* 1, no. 1 (1999): 55-68..
- [159] Veber, Daniel F., Stephen R. Johnson, Hung-Yuan Cheng, Brian R. Smith, Keith W. Ward, and Kenneth D. Kopple. "Molecular properties that influence the oral bioavailability of drug candidates." *Journal of medicinal chemistry* 45, no. 12 (2002): 2615-2623..
- [160] Siramshetty, Vishal B., Janette Nickel, Christian Omieczynski, Bjoern-Oliver Gohlke, Malgorzata N. Drwal, and Robert Preissner. "WITHDRAWN—a resource for withdrawn and discontinued drugs." *Nucleic acids research* 44, no. D1 (2016): D1080-D1086.
- [161] Liu, Jie, Kamel Mansouri, Richard S. Judson, Matthew T. Martin, Huixiao Hong, Minjun Chen, Xiaowei Xu, Russell S. Thomas, and Imran Shah. "Predicting hepatotoxicity using ToxCast in vitro bioactivity and chemical structure." *Chemical research in toxicology* 28, no. 4 (2015): 738-751.
- [162] Kroes, Robert, A. G. Renwick, M. Cheeseman, J. Kleiner, I. Mangelsdorf, A. Piersma, B. Schilter et al. "Structure-based thresholds of toxicological concern (TTC): guidance for

application to substances present at low levels in the diet." *Food and chemical toxicology* 42, no. 1 (2004): 65-83..

[163] Ames, Bruce N., William E. Durston, Edith Yamasaki, and Frank D. Lee. "Carcinogens are mutagens: a simple test system combining liver homogenates for activation and bacteria for detection." *Proceedings of the National Academy of Sciences* 70, no. 8 (1973): 2281-2285.

[164] Zhang, Luoping, Cliona M. McHale, Nigel Greene, Ronald D. Snyder, Ivan N. Rich, Marilyn J. Aardema, Shambhu Roy, Stefan Pfuhler, and Sundaresan Venkatachalam. "Emerging approaches in predictive toxicology." *Environmental and molecular mutagenesis* 55, no. 9 (2014): 679-688..

[165] Schrey, Anna K., Janette Nickel-Seeber, Malgorzata N. Drwal, Paula Zwicker, Nadin Schultze, Beate Haertel, and Robert Preissner. "Computational prediction of immune cell cytotoxicity." *Food and Chemical Toxicology* 107 (2017): 150-166..

[166] Frisch, M. J. E. A., G. W. Trucks, H. Bernhard Schlegel, Gustavo E. Scuseria, Michael A. Robb, James R. Cheeseman, Giovanni Scalmani et al. "gaussian 09, Revision d. 01, Gaussian." Inc., Wallingford CT 201 (2009).

[167] Jin, Z., Du, X., Xu, Y. et al. "Structure of M^{pro} from SARS-CoV-2 and discovery of its inhibitors". *Nature* 582, 289–293 (2020)

[168] Gao, Y., Yan, L., et al. " Structure of the RNA-dependent RNA polymerase from COVID-19 virus".(2020) *Science* 368: 779-782

[169] Berman, Helen M., Tammy Battistuz, Talapady N. Bhat, Wolfgang F. Bluhm, Philip E. Bourne, Kyle Burkhardt, Zukang Feng et al. "The protein data bank." *Acta Crystallographica Section D: Biological Crystallography* 58, no. 6 (2002): 899-907.

[170] Amalia, Intan Fitri, Assyifa Sayyidah, Kirana Aisyah Larasati, and Sarah Fadilah Budiarti. "Molecular Docking Analysis of α -Tomatine and Tomatidine to Inhibit Epidermal Growth Factor Receptor (EGFR) Activation in Non-Small-Cell Lung Cancer (NSCLC)." *JSMARTech: Journal of Smart Bioprospecting and Technology* 2, no. 1 (2020): 001-006.

[171] Darwin, K. Heran. "Is Required for Mycobacterium tuberculosis The Proteasome of." *Hum. Genet* 70 (2002): 1490.

[172] Bandyopadhyay, Nirmalya, Ankur Bikash Pradhan, Suman Das, Liping Lu, Miaoli Zhu, Shubhamoy Chowdhury, and Jnan Prakash Naskar. "Synthesis, structure, DFT calculations, electrochemistry, fluorescence, DNA binding and molecular docking aspects of a novel oxime

based ligand and its palladium (II) complex." *Journal of Photochemistry and Photobiology B: Biology* 160 (2016): 336-346.

[173] Guhathakurta, Bhargab, Pritha Basu, Chandra Shekhar Purohit, Nirmalya Bandyopadhyay, Gopinatha Suresh Kumar, Shubhamoy Chowdhury, and Jnan Prakash Naskar. "Synthesis, characterization, structure, DNA binding aspects and molecular docking study of a novel Schiff base ligand and its bis (μ -chloro) bridged Cu (II) dimer." *Polyhedron* 126 (2017): 195-204.

Chapter 5

Results & Discussion

5.1. ADMET screening

5.1.1. Physicochemical properties

The physicochemical properties such as solubility and lipophilicity play a major role of whether a drug can progress to be a successful drug candidate [174]. The lipophilicity property of the compounds portray an important role for molecular discovery activities in multifarious domains [175]. The parameters considered to measure the score are lipophilicity ($0.7 < XLogP < 5$), molecular weight (MW) ($150 < MW < 500$ g/mol), solubility ($0 < \log S < -6$). The physicochemical properties of our compounds are shown in Table 5.1. The results of the logP and logS values of all the designed compounds indicating, that they have a reasonable absorbency, showed the least lipophilicity and moderately water soluble except the compound FQ1 & FQ9 which are poorly soluble. Additionally, all compounds with limited complexity defined as fewer than 8 rotatable bonds except FQ3 and FQ4. Another physicochemical characteristic of great importance obtained with respect to the acid-base character of the molecule, determined by the ability to accept and donate protons H^+ [191]. Lipinski et al. [192] inferred that molecules that exhibit a lower number of hydrogen bond donor atoms - sum of hydrogen bond donor atoms O-H and N-H (HBD) and a higher number of hydrogen bond acceptor atoms - sum of hydrogen bond acceptor atoms O and N (HBA) have the most favorable ADME/Tox profile. In this Study all compounds have the higher number of hydrogen bond acceptor and lower number of hydrogen bond donor, so they have the most favorable ADMET profile.

Table 5.1. Physicochemicals Properties of compounds

Molecule	Water solubility (Log S)	Lipophilicity (Consensus Log $P_{o/w}$)	Molar refractivity	H-bond acceptor	H-bond donor	Rotatable bonds	Molecular Weight
FQ1	-6.60	1.88	118.49	6	3	6	498.7
FQ2	-5.25	2.60	129.28	5	2	7	521.77
FQ3	-5.23	2.91	137.45	5	1	8	547.81
FQ4	-4.88	3.06	146.54	5	0	9	573.85
FQ5	-4.69	2.49	129.28	5	2	7	521.77
FQ6	-5.01	2.65	128.37	5	2	7	521.77
FQ7	-5.19	2.47	122.89	5	2	6	504.75
FQ8	-5.04	2.34	120.20	5	3	6	495.74
FQ9	-6.03	2.36	114.94	5	3	5	478.71
FQ10	-4.81	2.23	120.20	6	3	6	495.74
FQ11	-5.13	2.55	119.29	6	3	6	495.74

FQ12	-5.31	2.20	113.81	6	3	5	478.71
FQ13	-5.15	2.24	111.11	6	4	5	469.70
FQ14	-4.98	2.67	118.18	4	2	6	479.74
FQ15	-5.11	2.95	117.35	3	2	6	463.74
FQ16	-5.26	2.71	122.07	4	2	6	488.75
FQ17	-5.09	2.90	127.55	4	2	7	505.77
FQ18	-4.63	2.82	127.26	4	1	7	505.77
FQ19	-5.37	2.88	128.46	4	2	7	505.77
FQ20	-4.59	2.48	119.37	5	3	6	479.7

5.1.2. Druglikeness and pharmacokinetics

- **Druglikeness**

According to Lipinski's rule of five[145],11 compounds (FQ1,FQ8,FQ9, FQ10, FQ11, FQ12, FQ13, FQ14, FQ15, FQ16, FQ20) had a good druglikeness satisfying all five criteria under this rule. This proves these ligands can serve as qualified drug candidates. According to Ghose's filter[146] ,6 compounds (FQ9, FQ12, FQ13, FQ14, FQ15, FQ20) had a good druglikeness implementing the four criteria under this rule. Also ,all the compounds had a good druglikeness depending on rule of Veber[147],characterized by high polarity($tPSA \leq 140$) ,and good flexibility(number of rotatable bonds ≤ 10).Same like Egan's filter ,all the ligands are highly druglikeness[148].the most important rules of drug likeness. e.g. Lipinski, Ghose, Veber, Egan, Muegge showed a score of 55%, indicating good bioavailability for all compounds which means a good druglikeness.Table 5.2,5.3

Table 5.2.Druglikeness properties of compounds

Molecule	Lipinski ≠violation	Ghose ≠violation	Veber ≠violation	Egan ≠violation	Muegge ≠violation	Bioavailability Score
FQ1	0	1	0	0	0	0.55
FQ2	1	1	0	0	0	0.55
FQ3	1	2	0	0	0	0.55
FQ4	1	2	0	0	0	0.55
FQ5	1	1	0	0	0	0.55
FQ6	1	1	0	0	0	0.55
FQ7	1	1	0	0	0	0.55
FQ8	0	1	0	0	0	0.55
FQ9	0	0	0	0	0	0.55
FQ10	0	1	0	0	0	0.55
FQ11	0	1	0	0	0	0.55
FQ12	0	0	0	0	0	0.55
FQ13	0	0	0	0	0	0.55
FQ14	0	0	0	0	0	0.55

FQ15	0	0	0	0	0	0.55
FQ16	0	1	0	0	0	0.55
FQ17	1	1	0	0	0	0.55
FQ18	1	1	0	0	0	0.55
FQ19	1	1	0	0	0	0.55
FQ20	0	0	0	0	0	0.55

• Pharmacokinetics

The drug development process includes ADMET evaluation. As the drug is absorbed by the system, it encounters several membrane barriers such as gastrointestinal epithelial cells; hepatocyte membrane, blood capillary wall, restrictive organ barriers (e.g. Blood-brain-barrier), glomerulus, and the target cell [186]. A molecule is said to be less skin permeant if the value of log K_p is more negative [187]. From the ADMET results Table 5.3, all compounds are found to be the least skin permeant K_p. The absorption of the molecule in the intestine is explained by the gastrointestinal (GI) parameter, it is reported as high which means all the compounds are highly absorbed in the intestine HIA. It is a physiological barrier which restricts the passage of most of the compounds from the blood to brain, thus having a brain protecting property [188]. The compound FQ15 was predicted to be blood-brain-barrier (BBB) permeant, and therefore, this compound may be suitable for central nervous system therapy, the rest show negative response for blood brain barrier (BBB). P-glycoprotein (P-gp) is an efflux drug transporter that serves as a biological barrier that protects cells from the harmful effects of drugs by transporting toxins and xenobiotics out of cells [189], also all of the compounds are substrates to P-gp except FQ3 and FQ4. In the family of CYP enzymes, the CYP3A4 was the most important enzyme on account of metabolizing 50% of all drugs by itself and the CYP2C9 enzyme mainly metabolizes several clinically used drugs such as celecoxib and diclofenac [190]. Almost all of the molecules returned as non-inhibitors for CYP isoenzymes except for FQ1 for CYP2C9 and FQ1 and FQ4 for CYP2C9, FQ16 for CYP3A4. The Boiled-egg plot between TPSA and LogP shown in Figure 5.1 allows to evaluate passive gastrointestinal absorption (HIA) and brain penetration (BBB), the white region is for high probability for passive absorption by GIT and the yellow region (yolk) is for high probability of brain penetration. In addition, the points are coloured in blue, if predicted as actively effluxed by P-gp (PGP⁺) and in red if predicted as non-substrate of P-gp (PGP⁻) [181]. In this study prediction, all compounds except FQ1 are within the prediction site, among them FQ15 is within the yolk (high brain penetration) of the BOILED-Egg and the rest are in the white of the

BOILED-Egg (high passive absorption of GIT).The FQ3 and FQ4 are depicted as red indicating non-substrate of P-gp,the rest in blue actively effluxes by P-gp .The

Table 5.3.Pharmacokinetics properties of compounds

Molecule	GI absorption	BBB permeant	P-gp substrate	CYP1A2 inhibitor	CYP2C19 inhibitor	CYP2C9 inhibitor	CYP2D6 inhibitor	CYP3A4 inhibitor	Log K_p (skin permeation) Cm/s
FQ1	High	No	Yes	No	Yes	Yes	No	No	-6.32
FQ2	High	No	Yes	No	No	No	No	No	-6.93
FQ3	High	No	No	No	No	No	No	No	-7.06
FQ4	High	No	No	No	No	Yes	No	No	-7.41
FQ5	High	No	Yes	No	No	No	No	No	-7.32
FQ6	High	No	Yes	No	No	No	No	No	-7.10
FQ7	High	No	Yes	No	No	No	No	No	-6.96
FQ8	High	No	Yes	No	No	No	No	No	-6.97
FQ9	High	No	Yes	No	No	No	No	No	-6.28
FQ10	High	No	Yes	No	No	No	No	No	-7.12
FQ11	High	No	Yes	No	No	No	No	No	-6.90
FQ12	High	No	Yes	No	No	No	No	No	-6.77
FQ13	High	No	Yes	No	No	No	No	No	-6.77
FQ14	High	No	Yes	No	No	No	No	No	-6.61
FQ15	High	Yes	Yes	No	No	No	No	No	-6.27
FQ16	High	No	Yes	No	No	No	No	Yes	-6.65
FQ17	High	No	Yes	No	No	No	No	No	-6.78
FQ18	High	No	Yes	No	No	No	No	No	-6.97
FQ19	High	No	Yes	No	No	No	No	No	-6.59
FQ20	High	No	Yes	No	No	No	No	No	-7.01

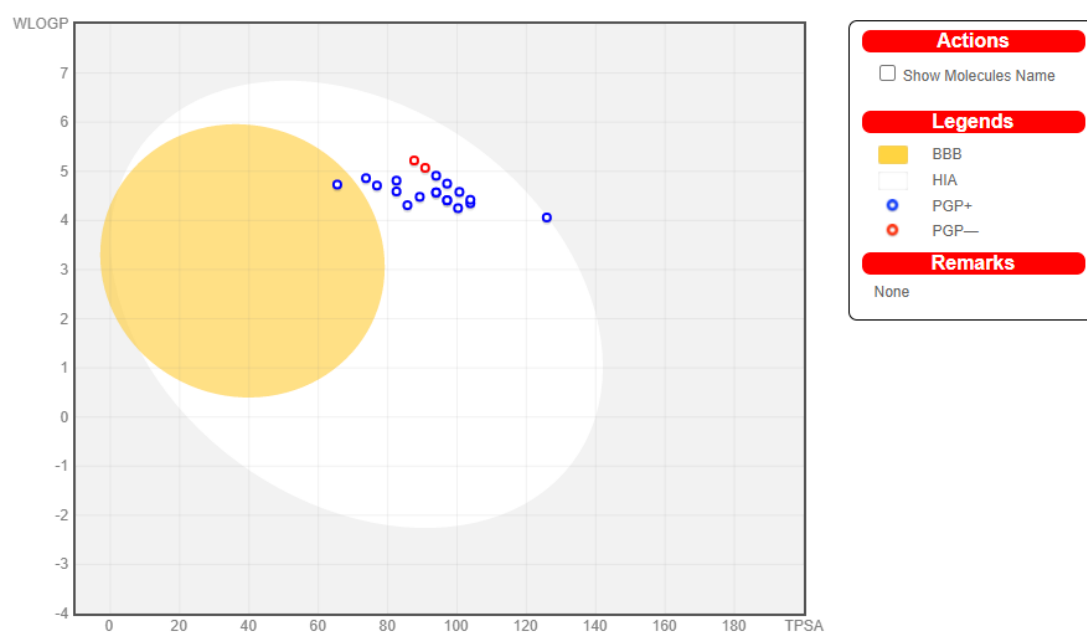


Figure 5.1.The Boiled-egg plot of compounds

- **Medicinal chemistry**

Similarly, these compounds showed no PAINS (Pan Assay Interference compounds or frequent hitters or promiscuous compounds) so the molecules shows potent response in assays irrespective of the protein targets, notably such compounds are reported to be active in many different assays, which can be considered as potential starting points for further exploration. On other hand all the compounds show 2 to 5 Brenk alert, considers compounds that are less smaller and more hydrophobic and not those defined by “Lipinski’s rule of 5” to widen opportunities for lead optimization. This was after exclusion of compounds with potentially mutagenic, reactive and unfavorable groups such as nitro groups, sulfates, phosphates, 2-halopyridines and thiols [176]. The concept of lead likeness designed to provide leads with tremendous affinity in high throughput screening (HTS) that allow for exploitation of additional interactions in the lead optimization phase. Leads are exposed to chemical modifications that will most likely decrease size and increase lipophilicity which is less hydrophobic than drug like molecules. Lead optimization has been done by rule based method consisting of molecules with molecular weight in between 250 and 350 Da, ClogP ≤ 3.5 and are greatly considered as superior to those of drug like compounds and therefore lead like [177,178]. All the compounds flouted Brenk’s rule, and all failed Leadlikeness criteria of molecular weight. All the newly designed compounds expose synthetic accessibility score in range of 3.70 to 4.02 suggesting that these compounds are facility synthesizable.

Table 5.4. Medicinal chemistry of compounds

Molecule	PAINS	Brenk	Leadlikeness	Synthetic accessibility (From 1 to 10)
FQ1	0	5	2	3.80
FQ2	0	3	2	3.86
FQ3	0	3	3	3.94
FQ4	0	2	2	4.02
FQ5	0	4	1	3.91
FQ6	0	4	1	3.84
FQ7	0	4	1	3.77
FQ8	0	4	1	3.75
FQ9	0	5	2	3.75
FQ10	0	3	1	3.79
FQ11	0	3	1	3.75
FQ12	0	3	1	3.72
FQ13	0	3	1	3.70
FQ14	0	4	2	3.76
FQ15	0	4	2	3.70
FQ16	0	3	2	3.67
FQ17	0	3	2	3.75

FQ18	0	4	1	3.92
FQ19	0	2	2	3.70
FQ20	0	3	1	3.71

5.1.4. The toxicity

The Protox online server also predicts five toxicological endpoints such as cytotoxicity, mutagenicity, carcinogenicity, hepatotoxicity, immunotoxicity. Toxicity classes are defined according to the globally harmonized system of classification of labelling of chemicals ([GHS](#)), The Hazard Communication Standard. LD50 values are given in [mg/kg]:

- class 1, fatal if swallowed ($LD50 \leq 5$)
- class 2, fatal if swallowed ($5 < LD50 \leq 50$)
- class 3, toxic if swallowed ($50 < LD50 \leq 300$)
- class 4, harmful if swallowed ($300 < LD50 \leq 2000$)
- class 5, may be harmful if swallowed ($2000 < LD50 \leq 5000$)
- class 6, non toxic ($LD50 \geq 5000$)

All compounds the LD50 surrounded 300 and 2000, so all belong into class 4 except FQ7, FQ14, FQ15 and FQ18 that belongs to class 3. The normally probability of prediction of toxicity model used ProTox-II webserver referenced below 0.7 so, all the compounds ranked immunotoxic active (red) because the probability of prediction is 0.85 to 0.99. Also all compounds are within the limit concerning the mutagenicity except FQ4 and FQ19. The rest results showed that all compounds were predicted to be non hepatotoxic, noncarcinogenic and noncytotoxic Table 5.5.

According to in silico physicochemicals, pharmacokinetics, druglikeness and medicinal chemistry prediction and toxicity prediction, the best ligands selected for the molecular docking study are FQ3, FQ5, FQ6, FQ9, FQ13, FQ16, and FQ19.

Table 5.5 Toxicity prediction of compounds

Molecule	Class	Cytotoxicity	Mutagenicity	Immunotoxicity	Carcinogenicity	Hepatotoxicity
FQ1	4	0.52	0.68	0.99	0.53	0.52
FQ2	4	0.51	0.58	0.99	0.63	0.59
FQ3	4	0.51	0.59	0.99	0.56	0.59
FQ4	4	0.55	0.51	0.85	0.60	0.61
FQ5	4	0.52	0.61	0.96	0.61	0.58
FQ6	4	0.55	0.63	0.99	0.58	0.56
FQ7	3	0.57	0.67	0.98	0.56	0.58

FQ8	4	0.53	0.66	0.99	0.60	0.55
FQ9	4	0.51	0.61	0.99	0.59	0.54
FQ10	4	0.50	0.68	0.98	0.60	0.58
FQ11	4	0.53	0.68	0.99	0.57	0.54
FQ12	4	0.53	0.68	0.99	0.58	0.56
FQ13	4	0.51	0.66	0.99	0.59	0.55
FQ14	3	0.57	0.69	0.99	0.51	0.58
FQ15	3	0.58	0.68	0.94	0.50	0.58
FQ16	4	0.58	0.67	0.87	0.52	0.60
FQ17	4	0.58	0.64	0.99	0.58	0.58
FQ18	3	0.53	0.66	0.89	0.50	0.61
FQ19	4	0.56	0.51	0.86	0.66	0.64
FQ20	4	0.50	0.63	0.98	0.59	0.58

5.2. Molecular docking

At the end of docking runs, diverse binding energies of the ligand were obtained with their respective conformations; the stable conformation, which corresponds to the lowest binding energy, was chosen as the best pose. The binding energy and binding constant K of the docked structures of all ligands with the two proteins are summarized in Table 5.6. The magnitude of the calculated binding energy indicates a high binding affinity between proteins and the studied ligands, the binding constant K was calculated using the equation:

$$\Delta G = -RT \ln K$$

Table 5.6 Binding free energies and binding constant values obtained by molecular docking approach

Compounds	6LU7		7BTF	
	- ΔG (Kcal/mol)	K (M ⁻¹)	- ΔG (Kcal/mol)	K (M ⁻¹)
FQ3	-10.6	57.7×10 ⁶	-6.48	55.53×10 ³
FQ5	-8.65	2.54×10 ⁶	-6.12	30.26×10 ³
FQ6	-10.24	31.44×10 ⁶	-6.3	40.99×10 ³
FQ9	-9.67	12.03×10 ⁶	-6.79	93.65×10 ³
FQ13	-8.1	0.852×10 ⁶	-6.19	34.06×10 ³
FQ16	-8.66	2.19×10 ⁶	-7.04	142.75×10 ³
FQ19	-9.58	10.33×10 ⁶	-6.47	54.6×10 ³

The results indicate that all the ligand have high binding affinity with studied receptor 6LU7, the best two are the ligands FQ3 and FQ6 with binding free energies equal to -10.6, -10.24 Kcal/mol respectively. Also, for the receptor 7BTF, the ligand FQ16 interacted the best with binding energy equal to -7.04 Kcal/mol. Moreover, the ligands FQ3, FQ6 and

FQ16 represents the highest binding constant values K . The chosen ligand interacts with both receptors via hydrogen bonds and a hydrophobic bond Figure 5.2

The ligands interactions information with 6LU7 and 7BTF are summarized in Table 5.7

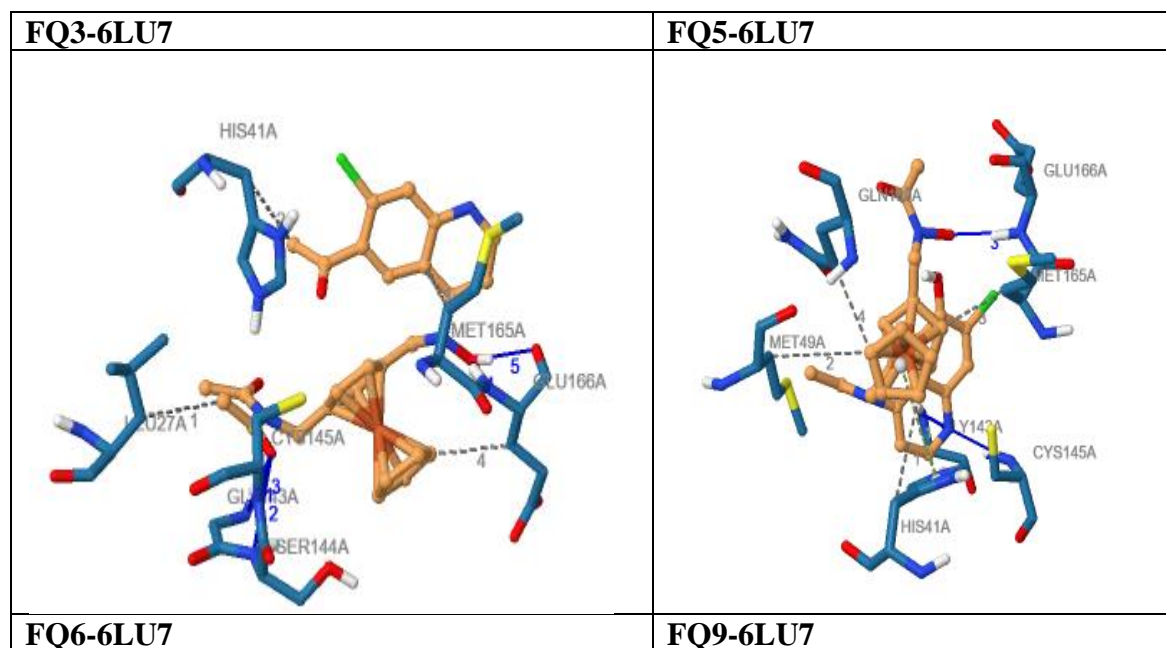
The results showed that all compounds interacted via hydrogen bonds to the amino acids of the binding pocket of 6LU7. The best ligands FQ13 interacted via three hydrogen bonds to Arg180, Thr190 and Thr190 amino acids of 6lu7 and Three hydrophobic bonds between the ligand and Pro168, Gln189 and Gln189 of amino acids of 6Lu7. Also, the results showed that all compounds interacted via hydrogen and hydrophobic bonds of 7BTF.

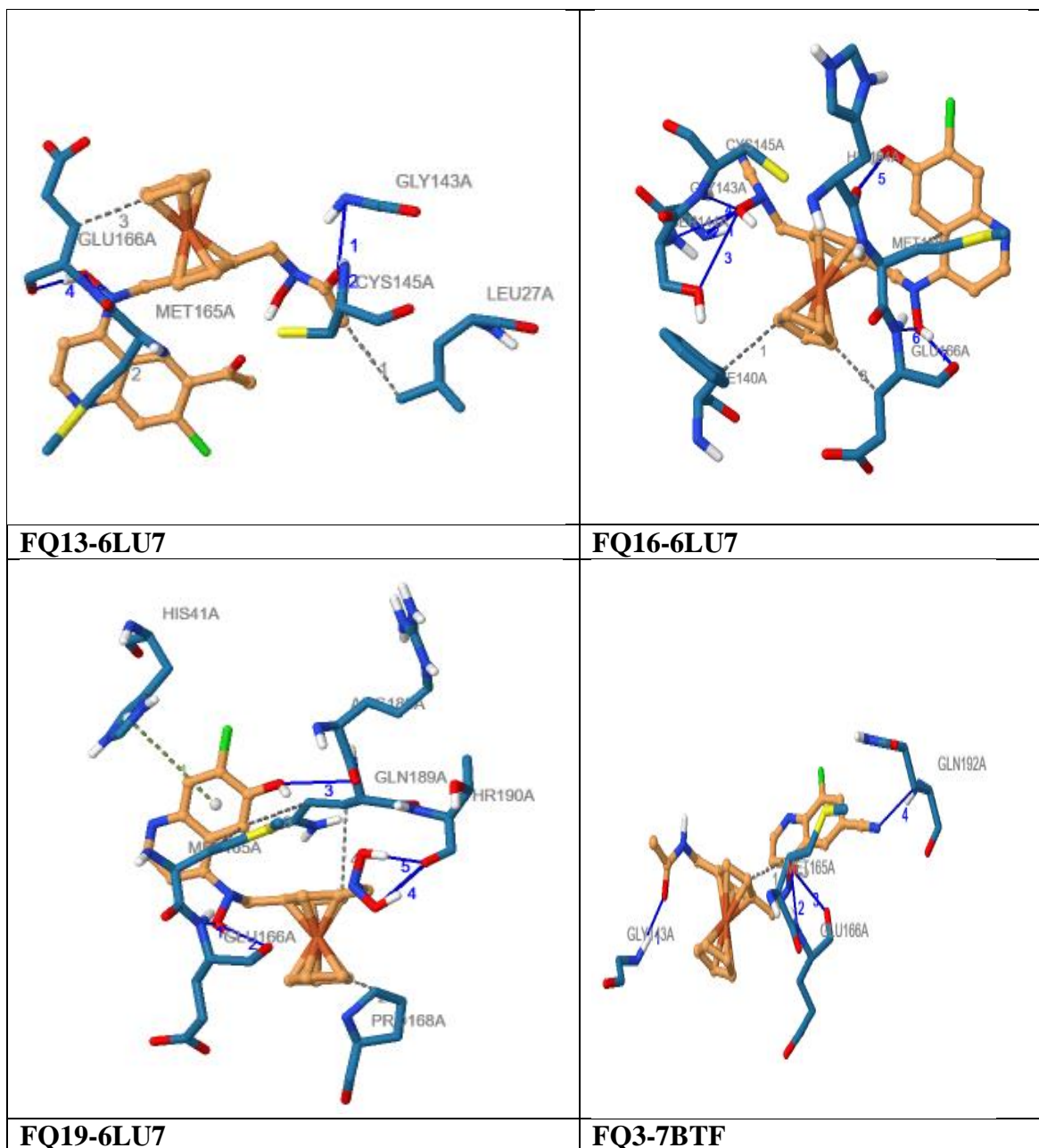
Table 5.7 Distances of formed bonds between ligands and 6LZG and 7BTF receptor's residues

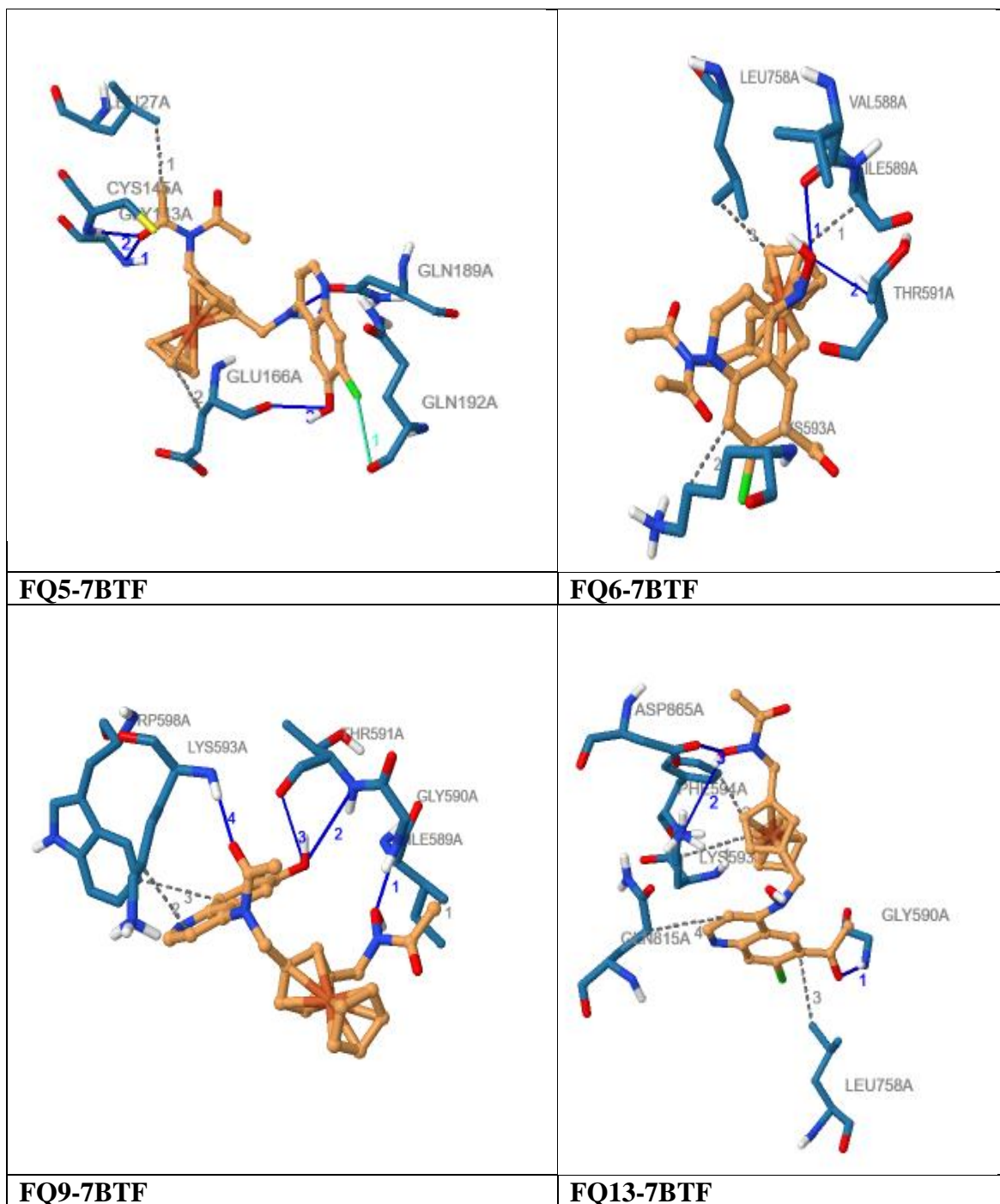
Adduct	Bond type	AA	Distance
FQ3-6LU7	Hydrophobic interactions	LEU27A	3.78
		HIS41A	3.91
		MET25A	3.23
		GLU166A	3.16
	Hydrogen-bonds	GLY143A	2.99
		SER144A	3.18
		CYS145A	3.0
		GLU166A	3.05
FQ5-6LU7	Hydrophobic interactions	GLU166A	2.17
		HIS41A	3.62
		MET49A	3.93
		MET165A	3.12
	Hydrogen-bonds	GLN189A	3.23
		GLY143A	2.99
		CYS145A	2.88
FQ6-6LU7	Hydrophobic interactions	GLU166A	2.86
		LEU27A	3.89
		MET165A	3.12
	Hydrogen-bonds	GLU166A	3.03
		GLY134A	3.06
		CYS145A	2.77
FQ9-6LU7	Hydrophobic interactions	GLU166A	3.52
		GLU166A	2.68
		PHE140A	3.98
	Hydrogen-bonds	MET165A	3.03
		GLU166A	3.34
		GLY143A	2.82
		SER144A	2.85
		SER144A	4.09
		CYS145A	2.81
Hydrophobic interactions	HIS164A	3.17	
	GLU166A	3.07	
	GLU166A	2.70	
	Hydrophobic interactions	MET165A	3.28
		PRO168A	3.42
		GLN189A	3.75

FQ13-6LU7		GLN189A	3.99
	Hydrogen-bonds	GLU166A	2.68
		GLU166A	3.07
		ARG188A	3.11
		THR190A	2.82
		THR190A	2.54
FQ16-6LU7	Hydrophobic interactions	MET165A	3.48
	Hydrogen-bonds	GLY134A	2.98
		GLU166A	2.76
		GLU166A	2.87
		GLN192A	3.21
FQ19-6LU7	Hydrophobic interactions	LEU27A	3.41
		GLU166A	3.40
	Hydrogen-bonds	GLY143A	2.82
		CYS145A	3.01
		GLU166A	2.81
		GLN189A	2.72
FQ3-7BTF	Hydrophobic interactions	ILE589A	3.13
		LYS593A	3.17
		LEU758A	3.30
	Hydrogen-bonds	VAL588A	2.44
		THR591A	2.98
FQ5-7BTF	Hydrophobic interactions	ILE589A	3.19
		LYS593A	3.21
		TRY598A	3.41
	Hydrogen-bonds	GLY590A	2.64
		THR591A	3.51
		THR591A	2.98
FQ6-7BTF	Hydrophobic interactions	LYS593A	3.70
		PHE594A	3.31
		LEU758A	3.40
		GLN815A	3.82
	Hydrogen-bonds	GLY590A	2.87
		LYS593A	4.08
		ASP865A	3.56
FQ9-BTF	Hydrophobic interactions	LYS593A	3.23
		TRP598A	3.31
	Hydrogen-bonds	GLY590A	2.87
		THR591A	2.85
		LYS593A	4.08
		CYS813A	2.88
Hydrophobic interactions	SER814A	2.81	
	LYS593A	3.67	
		TRP598A	3.53

FQ13-7BTF	Hydrogen-bonds	LEU758A	3.33
		VAL588A	3.80
		VAL588A	3.10
		GLY590A	3.30
		LYS593A	2.64
		ASP865A	3.16
FQ16-7BTF	Hydrophobic interactions	PHE441A	3.25
		ILE548A	3.43
		ILE548A	3.77
		ILE548A	3.16
		ILE548A	3.89
		ARG836A	3.83
		ALA840A	3.52
	Hydrogen-bonds	ARG858A	3.75
		HIS439A	3.14
		ARG836A	3.24
FQ19-7BTF	Hydrophobic interactions	ASP845A	2.79
		PHE441A	3.52
		ALA547A	3.87
		ILE548A	3.75
		VAL844A	3.20
		ASP845A	3.55
	Hydrogen-bonds	ARG858A	3.93
		TYR546A	3.81
		ASP845A	2.71
		ASP845A	3.30
		ARG858A	3.31
		ARG858A	3.30







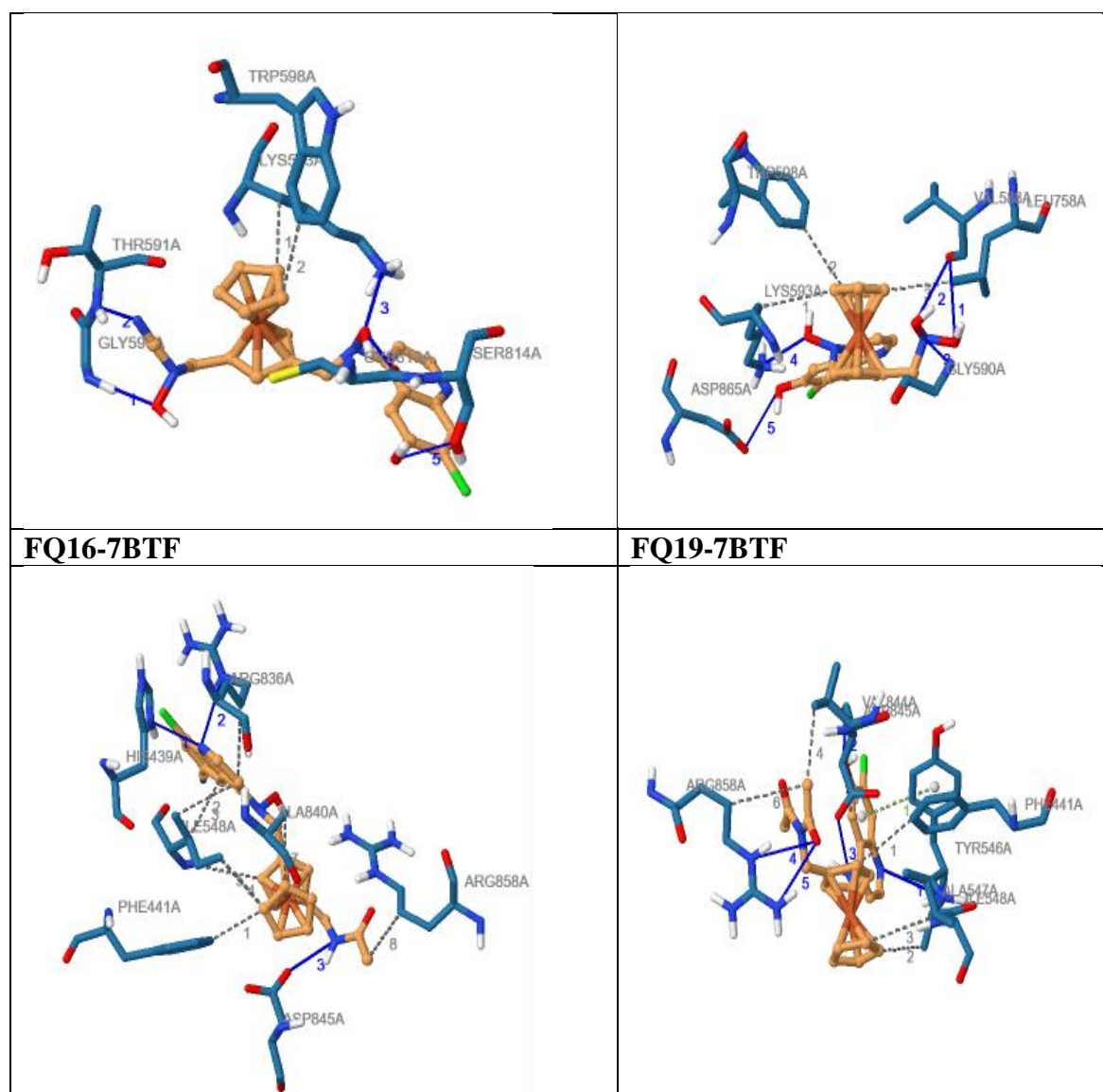


Figure 5.2:3D interaction between the studied ligands and the targets 6VSB and 6LZG where the grey lines show hydrophobic bonds and the blue lines show the H-bonds

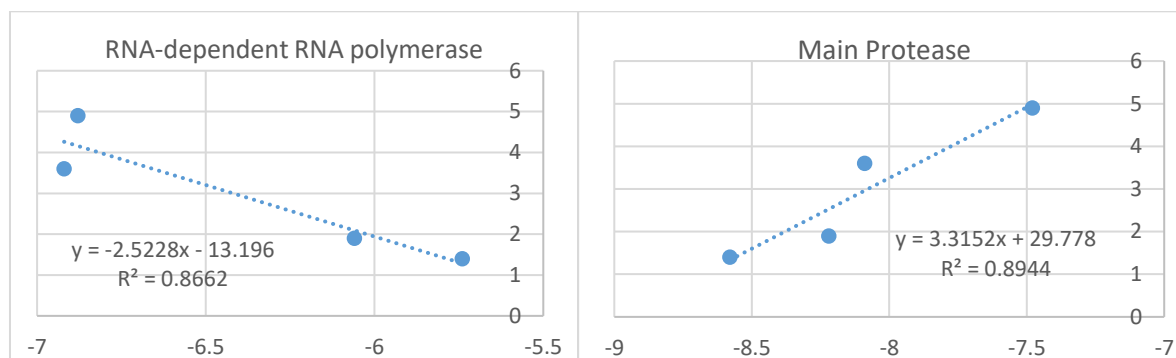
5.3. Prediction of inhibitory concentration IC₅₀

After the docking study, we attempted to predict the IC₅₀ of the lead compounds. The docking results of reference compounds as well as their IC₅₀ values against SARS-COV are shown in Table 5.8. The linear regression analysis showed a good correlation with correlation coefficient equal to 0.86 and 0.89 respectively with the enzymes RNA-dependent RNA polymerase (7BTF) and Mpro protein (6LU7).

The predicted IC₅₀ values for the lead compounds were in the range of -5.363 to 2.924 mM and from 2.24 to 4.564 for Mpro protein and RdRp respectively, which were comparatively similar to the IC₅₀ of standard compounds that range between 1.4 to 4.9 mM.

Table 5.8. Binding free energies and IC50 of standard compounds values obtained by molecular docking approach

FQ	ΔG (6LU7)	ΔG (7btf)	IC50
F1	-8.58	-5.74	1.4
F2	-9.47	-6.88	4.9
F3	-8.22	-6.06	1.9
F4	-8.09	-4.86	3.6

**Figure 5.3.** The difference between binding free energies and IC50 of compounds values obtained by molecular docking approach.**Table 5.9.** binding free energies and IC50 of compounds values obtained by molecular docking approach

Comps	6LU7		7BTF	
	ΔG (6LU7)	IC50	ΔG	IC50
FQ3	-10.6	-	-6.48	3.151744
FQ5	-8.65	1.101	-6.12	2.243536
FQ6	-10.24	-	-6.3	2.69764
FQ9	-9.67	-	-6.79	3.933812
FQ13	-8.1	2.924	-6.19	2.420132
FQ16	-8.66	1.068	-7.04	4.564512
FQ19	-9.58	-	-6.47	3.126516

References:

[174] Kwong, Elizabeth, ed. Oral formulation roadmap from early drug discovery to development. John Wiley & Sons, 2017.

[175] Pliška, V., Bernard Testa, and Han van de Waterbeemd. "Lipophilicity: The empirical tool and the fundamental objective. An introduction." *Lipophilicity in drug action and toxicology* (1996): 1-6. [177] Hann, Michael M., and György M. Keserü. "Finding the sweet spot: the role of nature and nurture in medicinal chemistry." *Nature reviews Drug discovery* 11, no. 5 (2012): 355-365.

[178] Hann, Michael M., and György M. Keserü. "Finding the sweet spot: the role of nature and nurture in medicinal chemistry." *Nature reviews Drug discovery* 11, no. 5 (2012): 355-365.

[176] Brenk, Ruth, Alessandro Schipani, Daniel James, Agata Krasowski, Ian Hugh Gilbert, Julie Frearson, and Paul Graham Wyatt. "Lessons learnt from assembling screening libraries for drug discovery for neglected diseases." *ChemMedChem* 3, no. 3 (2008): 435.

[181] Daina, Antoine, and Vincent Zoete. "A boiled-egg to predict gastrointestinal absorption and brain penetration of small molecules." *ChemMedChem* 11, no. 11 (2016): 1117.

[186] Alam, Sarfaraz, Sadaf Nasreen, Ateeque Ahmad, Mahendra Pandurang Darokar, and Feroz Khan. "Detection of natural inhibitors against human liver cancer cell lines through QSAR, Molecular Docking, and ADMET studies." *Current Topics in Medicinal Chemistry* (2021).

[187] Potts, Russell O., and Richard H. Guy. "Predicting skin permeability." *Pharmaceutical research* 9, no. 5 (1992): 663-669.

[188] Nisha, Chaluveelaveedu Murleedharan, Ashwini Kumar, Archana Vimal, Bhukya Mounika Bai, Dharm Pal, and Awanish Kumar. "Docking and ADMET prediction of few GSK-3 inhibitors divulges 6-bromoindirubin-3-oxime as a potential inhibitor." *Journal of Molecular Graphics and Modelling* 65 (2016): 100-107.

[189] Brunton, L., Chabner, B., &Knollman, B. (2011). *Goodman and Gilman's the pharmacological basis of therapeutics*. 12th ed. McGraw-Hill Education/Medical.

[190] Daina, Antoine, Olivier Michielin, and Vincent Zoete. "SwissADME: a free web tool to evaluate pharmacokinetics, drug-likeness and medicinal chemistry friendliness of small molecules." *Scientific reports* 7, no. 1 (2017): 1-13.

[191] Avdeef, Alex. *Absorption and drug development: solubility, permeability, and charge state*. John Wiley & Sons, 2012.

[192] Lipinski, Christopher A., Franco Lombardo, Beryl W. Dominy, and Paul J. Feeney. "Experimental and computational approaches to estimate solubility and permeability in drug discovery and development settings." *Advanced drug delivery reviews* 23, no. 1-3 (1997): 3-25.

Conclusion

In the present study, *in silico* approaches applicable for the molecules of ferroquine and study their effects on the main protease and the RNA polymerase of SARS-COV2. After forming the combinatorial library on Smilib v2.0 by substitution of the roots NO₂, CN, SCH₃, OH and COCH₃ on the base core of ferroquine, 625 compounds were obtained. Virtual screening was performed using SwissADME and ProTox web servers, 20 compounds were selected, the ADMET properties were obtained which indicated a good druglikeness, pharmacokinetics, and physicochemicals properties. The toxicity prediction showed that all compounds are immunotoxic, and the most within the limit of mutagenicity, however all compounds were predicted to be non-hepatotoxic, noncarcinogenic and noncytotoxic.

After the ADMET virtual screening, 7 compounds which showed better ADMET properties were selected for the molecular docking study. The compounds were docked into the main protease and the RNA polymerase of SARS-COV2. The two compounds FQ3 and FQ6 with binding free energies equal to -10.6 and -10.24 Kcal/mol respectively are the best ligands interacted with the main protease. For the receptor RNA polymerase, the ligand FQ16 interacted the best with binding energy equal to -7.04 Kcal/mol. The best ligand FQ13 interacted via three hydrogen bonds to Arg180, Thr190 and Thr190 amino acids and three hydrophobic bonds between the ligand and Pro168, Gln189 and Gln189 amino acids of main protease, while all other compounds interacted via only hydrogen bonds to receptors. All ligands can be competitive inhibitors for receptors.

Furthermore, the IC₅₀ values of new compounds were predicted using linear regression which were in the range from -5,363 to 2,924 for the main protease, and from 2,433 to 4,564 for the RNA polymerase.

Finally, the studied compounds might be a good drug candidate for SARS-COV-2.